Synthesis and Characterisation of a Chiral Silica Aerogel

DISSERTATION ZUR ERLANGUNG DES DOKTORGRADES DER NATURWISSENSCHAFTEN (DR. RER. NAT.) DER FAKULTÄT CHEMIE DER UNIVERSITÄT REGENSBURG

vorgelegt von

Björn-Michael Bartel

aus Regensburg

2013

Synthesis and Characterisation of a Chiral Silica Aerogel

DISSERTATION ZUR ERLANGUNG DES DOKTORGRADES DER NATURWISSENSCHAFTEN (DR. RER. NAT.) DER FAKULTÄT CHEMIE DER UNIVERSITÄT REGENSBURG

vorgelegt von

Björn-Michael Bartel aus Regensburg

2013

Promotionsgesuch eingereicht am: Dienstag, 4. Juni 2013
Die Arbeit wurde angeleitet von: Professor Werner Kunz
Prüfungsausschuß:

Vorsitz:	Professor Sigurd Elz
1.Gutachter:	Professor Werner Kunz
2.Gutachter:	Apl. Professor Reinhard Rachel
3. Prüfer:	Professor Georg Schmeer

Contents

Introduction:....3
Aim of this Work:....3
History:....3
Properties:....6
Possible and Actual Applications of Aerogels:....10
Aerogel Synthesis in Theory:....12
Hydrolysis of Alcoxysilanes:....12
Condensation Reactions:....13
From Condensation over Particles to Gel Formation:....14
Ageing of Silica Structures:....15
Drying:....15
Freeze Drying:....17
Supercritical Drying:....18
Building the Autoclave:....24
Autoclave Operation Instructions:....30
Influencing Silica Growth:....34
Approach in Natural Systems:....34
Surface Active Substances....36
Synthesis of the Surfactant....38
Gel Forming....41
Drying....41
Heat Treatment....42
Analysis Methods:....43
Rotational Angle Measurement:....43
Aerogels as Rotational Angle Measurement Samples:....43
CD-Spectroscopy:....44
Aerogels as CD-Spectroscopy Samples:....44
Gaschromatography:....45
Aerogels as GC-Samples:....46
BET Measurements:....47
Aerogels as BET-Samples:....48

IR-Measurements:.....49
Aerogels as IR-Samples:.....50
Transmission Electron Microscopy:.....51
Aerogels as Transmission Electron Microscopy Samples:.....53
Scanning Electron Microscopy:.....54
Aerogels as Scanning Electron Microscopy Samples:.....56
Results of Template Based Aerogels Compared to Reference Aerogels 58
Conclusions.....66
Sorption:.....67
COSMO: The Conductor like Screening Model.....69
COSMO-RS: A Calculation Method for Intermolecular Interactions.....72
Adsorption on Silica Aerogels as Predicted by COSMO-RS σ-Moments.....75
The Investigated Systems.....76
Adsorption Measurements.....76
Derivation of the Working Equation for the Prediction of Adsorption Values..77
Interpretations.....81
Conclusions.....85
Conclusions and Outlook.....86
Acknowledgements.....89
References.....90
Appendices.....94
Sources and Copyright of some Figures:.....100
List of some Chemicals:.....102

Introduction:

Aim of this Work:

It is the aim of this work to modify silica aerogel to get a chiral silica based product. To achieve this several steps have to be achieved. As silica aerogels need special processing, to prevent shrinkage and deformation during drying, supercritical drying under pressure in an autoclave is necessary. There was no autoclave fit to this task available in the laboratory, so one was built as part of this work. It is further necessary to characterise the silica aerogel products and determine some of its properties. For this several measurement methods are necessary. Due to the unique and sometimes brittle nature of aerogels some measurement methods must be adapted to the aerogel material. A special emphasis is put on sorption properties of the silica aerogel. It is the aim to get sorption data through measurements and predict the sorption of different molecules on silica aerogels. For this equations are developed from the COSMO-RS approach. It is further an aim to characterise the surface of the aerogel by employing the equations from empirical measurements with the use of the σ-moments of the COSMO-RS approach.

History:

In the beginning of working on a topic stands a closer look on what has been done in that direction and what is already known. The topic of silica aerogels is no exception to that. It is a part of larger fields as silica gels and closely related to other topics such as silica xerogel or thin films prepared from amorphous silica. All this topics are part of the broad topic of amorphous silica. According to Sol-Gel-Science[1] from

Brinker and Scherer metal alcoxides as amorphous silica gels date back to 1846 when J. J. Ebelmen first described metal alcoxides from silicate trachloride that gelled through exposure to air in Justus Liebigs Annalen der Chemie. This broad spectrum of amorphous silica reaches from minerals as opals over biomineralisation and composite materials to glass industry to name only a few of the more prominent fields of research.

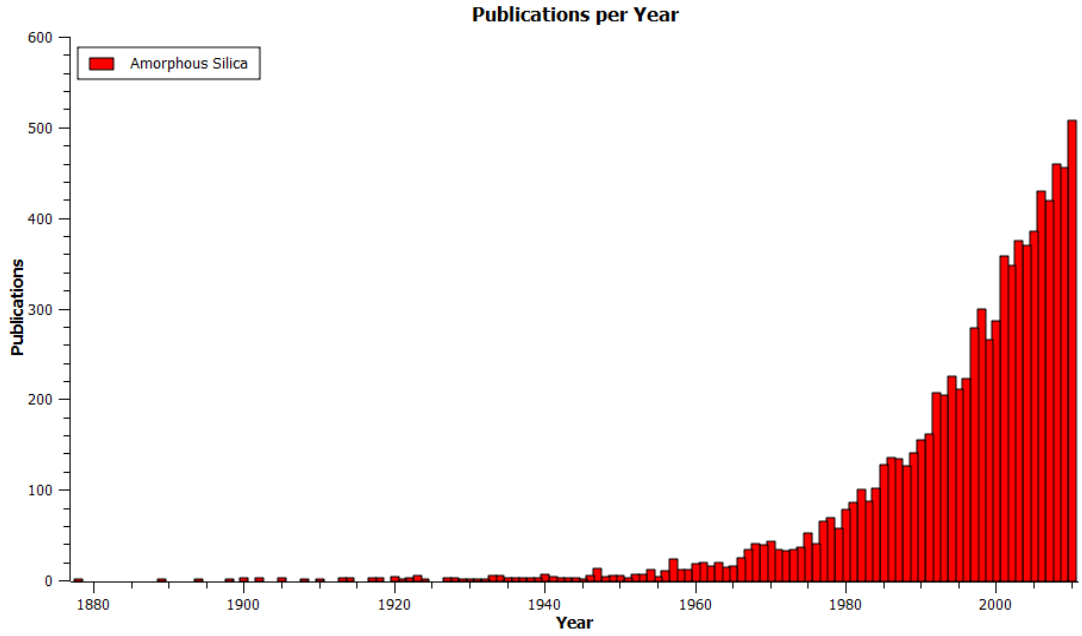

Figure 1: Publications per year for amorphous silica.

These fields are too broad and sometimes unrelated to the field of amorphous silica aerogels to contribute in a reasonable way. Sticking to silica aerogels and closely related fields in terms of amorphous silica growth and shape control such as silica xerogels, we come to a much more manageable amount of sources. It is to note that xerogels are partly synthesized in similar ways to aerogels but are different in many properties of these materials. According to literature databases of SciFinder the older publications in this fields date back to 1934, where the first production of aerogels

was reported. A search on the amount of publications per year leads to figures 1 and 2. The diagram in figure 2 clearly shows some changes of interest in the displayed fields of silica aerogel and silica xerogel. The first change is around the year of 1984 where interest in both fields started to increase. The second change affects silica xerogel around the year of 2004 since when there seems to be a stagnation of the number of publications per year while silica aerogel publication numbers still increase.

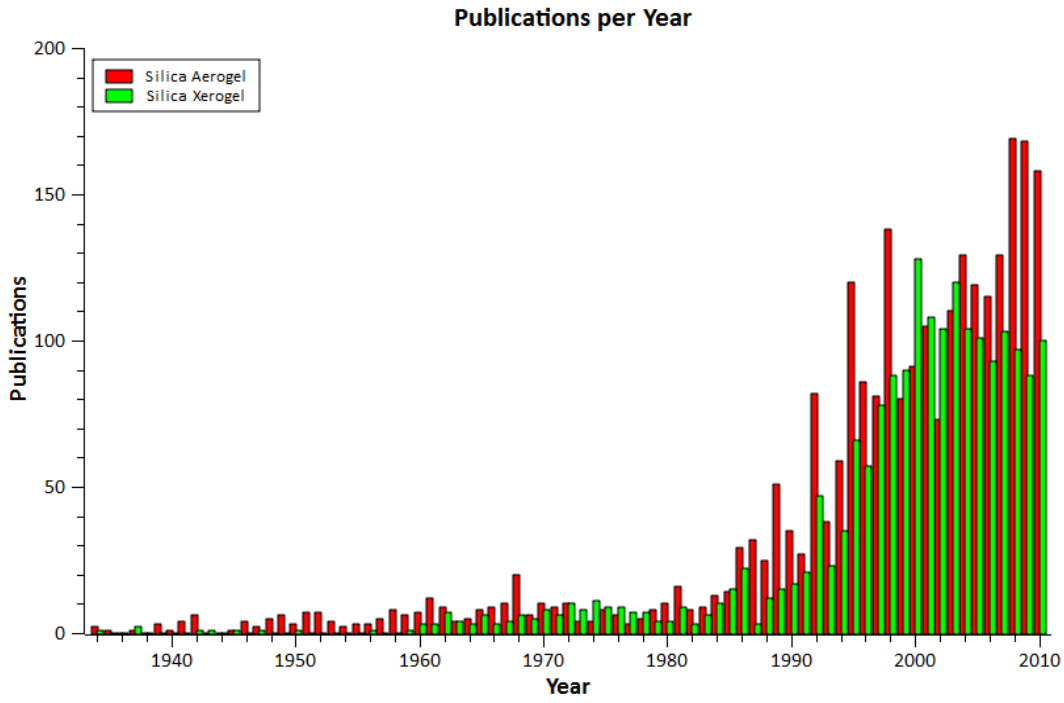

Figure 2: Publications per year for silica aerogels and silica xerogels.

The ongoing increase of publications about silica aerogels clearly states that it is still a field of current research. This might be due to the special and interesting properties of aerogels and despite or perhaps even more because of the still unsolved problems of very high production costs.

The first introduction of aerogels was made by Kistler et al. in the year of 1931.[2] There he showed methods for removing the liquid part of several gels through supercritical drying avoiding the shrinking and deformation of gels during common drying. Common drying leads to shrinked, so-called xerogels. The new material was examined in the following years and has unique properties that further propelled the interests in the field.

Properties:

Aerogels and silica aerogels have achieved many records for several properties. The most prominent record is for sure the one of the lowest density of a solid material. This originates from the structure of the gel. The liquid phase of the gel is exchanged with a gas phase resulting in a possible mass loss of over 90% resulting in a plain porous solid phase. The adaptable pore sizes are also a special property of the aerogel class of materials. The pores and spaces formerly filled with liquid now contribute to a high surface area. These spaces between the rigid silica material are also the reason for the extremely low density of aerogels.

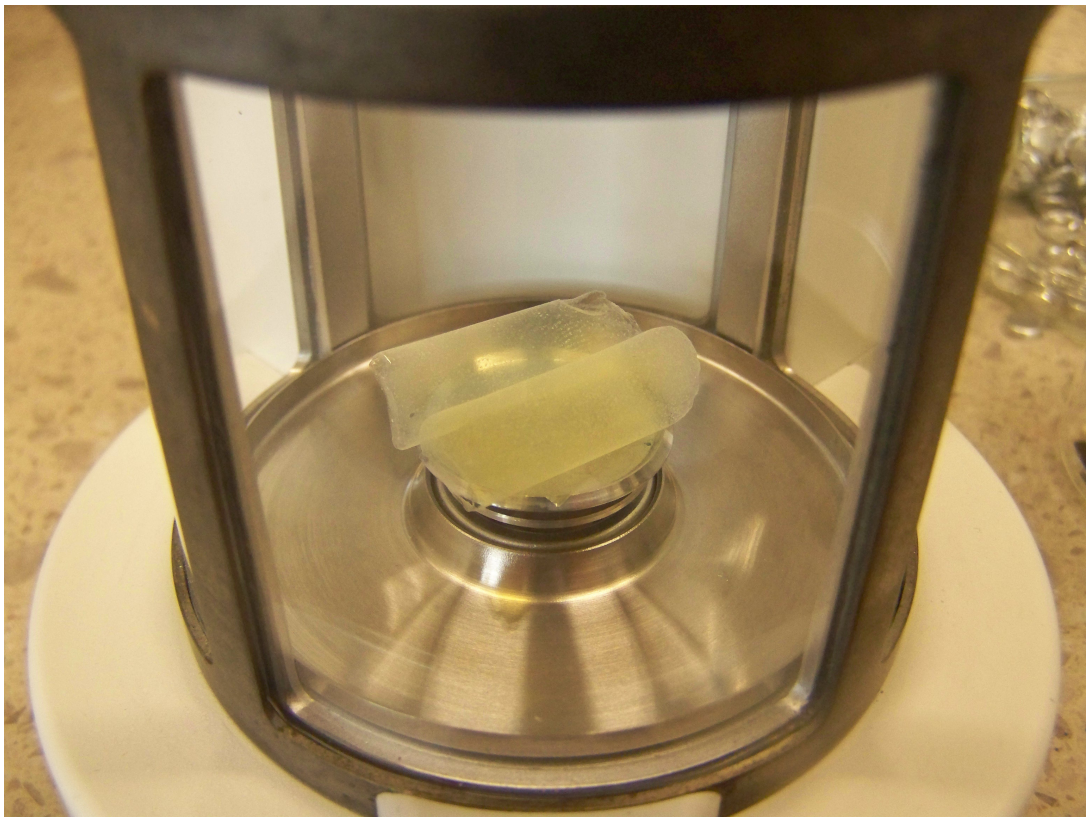

Figure 3: The transparent aerogel on this balance weights only 518.3 mg.

The glass like chemical structure of amorphous silica aerogels make them chemically resistant and the surface adaptable. The open gas filled solid network structure is also a reason for the thermal insulating feature of aerogels.

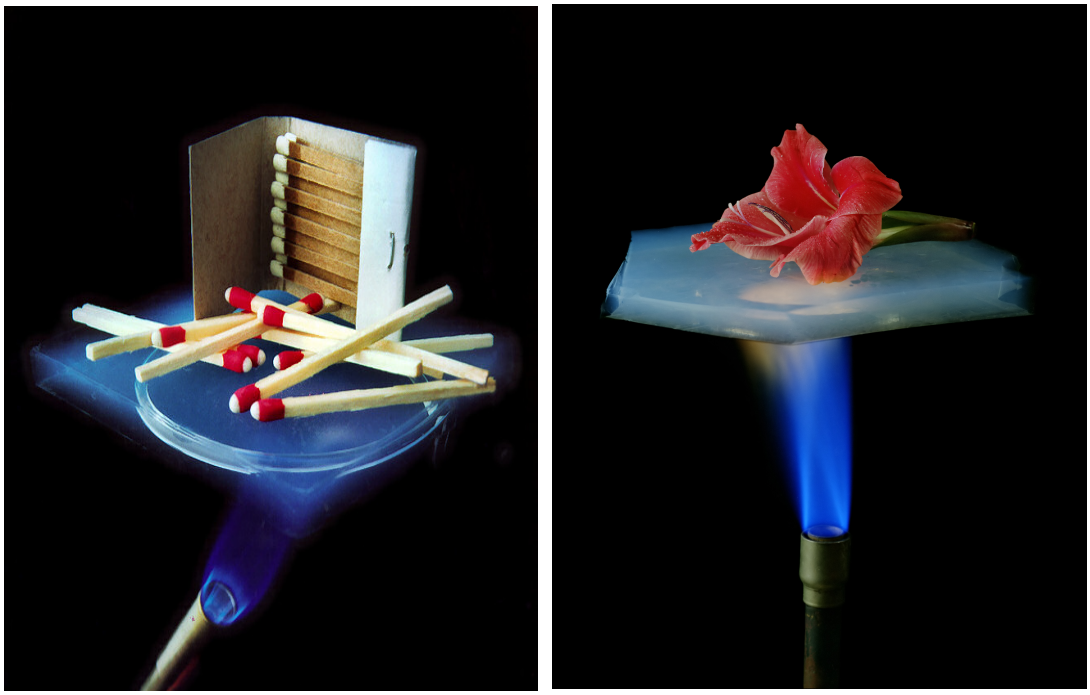

Figures 4a and b: Showing thermal isolating properties of aerogel.

Another interesting property is the transparency of amorphous silica aerogel, which is the result of the pore sizes that are small enough to let most light through. However light scattering does occur especially with blue light, due to its structure. So amorphous silica aerogel appears slightly blue and if the light source is directly behind the aerogel it looks yellowish. When handling silica aerogel and a solid block of this material falls down, there is some noise when it hits another hard surface. This noise comes from the shear forces inside the block. Considering its low density it is astonishing how stable aerogel blocks are when it comes to bear heavy loads.

Figure 5: Showing a 2.5 kg brick on top of a 2 g aerogel.

In terms of stability there is also a drawback that results from the difficulties in aerogel production. Silica aerogels can be unstable when it comes to capillaric forces that reach enormous values due to the small pore sizes. According to the book Sol–Gel–Science[1] from Brinker and Scherer on page 465, the values are in the range of 30 to 2000 bar.

Possible and Actual Applications of Aerogels:

Now that we had a look on the interesting and special properties of aerogels and especially amorphous silica aerogels, it should be clear that aerogels are promising high-tech materials. Due to their higher production costs they are mainly used when no other material can fulfil the task or when functionality is more important than costs. As energy efficiency is most important these days one of the most intriguing applications of the outstanding properties of silica aerogels combines its optical transparency with its thermal insulation. So it would be best, if these aerogels could be incorporated as thermal insulation in windows. However, beside the already mentioned costs, there is a problem with light scattering of blue light resulting in a slight blue color of the aerogel if illuminated with indirect light and a bright yellow colour of light that directly shines through the aerogel. Thus limiting insulating aerogel windows to special applications where thermal insulation is crucial for windows. The big surface area, on the other hand make this kind of material interesting in solar industry.[3] One of the most used applications in the form of a medium with special optical properties is that of cherenkov detectors.[4] In these detectors radioactive radiation is transformed to visible light that is used to measure the activity of nuclear fuel rods and whole nuclear reactors. There has also been research for silica aerogels as nuclear waste storage matrix.[5,6] Another idea of aerogel application is a safe container for gases due to the open porous structure of this material class. In this field the adsorption and desorption properties of aerogels can play an important role. These properties are also most important for aerogels as drug delivery systems. This is only possible due to the non toxic and inert properties of silica aerogels. Aerogels can be tuned to dissolve in moist environments and so

release adsorbed substances such as drugs.[7,8] Despite being chemically non toxic it has been shown that they can be used as insecticides due to their physical properties.[9] The aerogel in powdered form acts as an abrasive to the insects exoskeleton. A very special use of aerogels was to decelerate and collect high velocity dust from space without deforming or destroying the dust particles.[10,11]

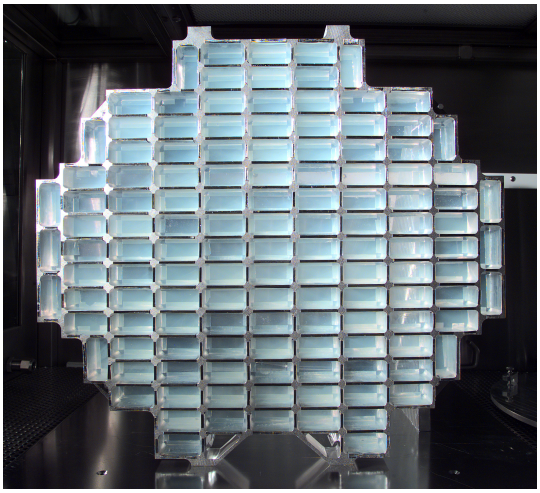

Figures 6a and b: NASA stardust collector and particle captured in aerogel.

But there are more widespread uses of aerogels as a dampening and filling material in tennis and squash rackets. Aerogels also improve electronics by allowing smaller compacter sizes of capacitors with the same capacitance.[12]

Aerogel Synthesis in Theory:

In order to explain synthesis of silica aerogels in detail some background knowledge on hydrolysis and condensation of silica gel precursors is important. So I will give a short introduction on this topic based on the book Sol – Gel – Science by C. Jeffrey Brinker and George W. Scherer.[1]

In principle there are two possible starting points for most silica chemistry which is first the solubilisation of Na_2SiO_3 in diluted acid as hydrochloric acid to form aqueous solution of $Si(OH)_4$. The other precursor is $Si(Cl)_4$ which can directly react with water to form $Si(OH)_4$ or react with alcohols to form alcoxysilanes or mixtures of both. It is most common to start with simple commercially available reagents of tetraalkoxysilanes such as tetramethoxysilane (TMOS) or tetraethoxysilanes (TEOS).

Forming of silica based gels as here presented is basically done in three steps. First solubilisation or at least mixture of the precursor with solvent and possible catalysts. A second step is condensation of the solubilised precursors resulting in dimers, oligomers and gel structures. Finally there is also an optional but preferable step of gel ageing that rigidifies the solid gel phase.

Hydrolysis of Alcoxysilanes:

There are two possibilities of exchanging an alcoxygroup (OR) with a hydroxy group (OH) in alcoxysilanes which depend on the pH of the solution. Note that the rate of hydrolysis is dependent on pH with a minimum in the neutral range of pH 7.

$$(RO)_3\text{-Si-OR} + H_2O \rightarrow (RO)_3\text{-Si-OH} + ROH$$

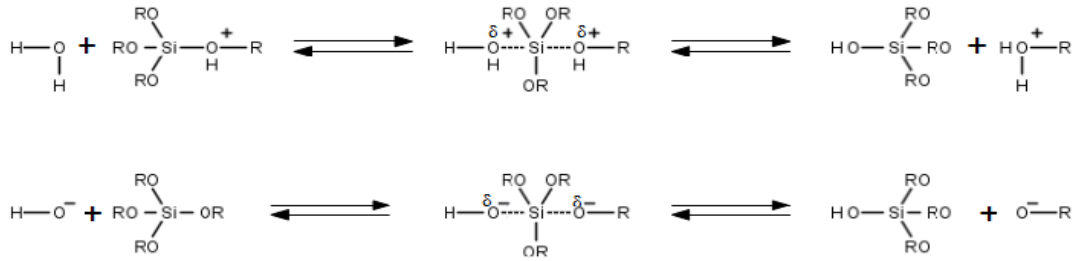

Figure 7: Reaction scheme for hydrolysation.

In acidic as in basic conditions the reaction mechanism is accordingly a S_N2-Reaction (Figure 7). The difference during acidic catalysis is that the silica alcoxane is protonated first.

Condensation Reactions:

The important part of particle growth and fusion of particles and whole networks to gels is the condensation reaction. This kind of connection can take place with either fully or partly hydrolysed silica alcoxanes. In case of two fully hydrolysed silica alcoxanes, these silica hydroxides both contribute one hydroxide group to form a silica oxygen bridge and a water molecule.

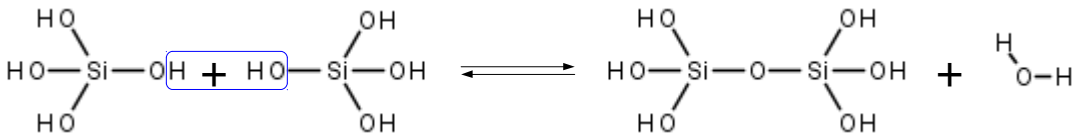

Figure 8: Reaction scheme showing the condensation reaction of fully hydrolysed silica with the so called lasso-chemistry.

In case of a partly hydrolysed system a hydroxy group can also react with an alcoxy group of another reactant to form a silica oxygen bridge and the corresponding

alcohol. This is the same result as it would have been with another hydrolisation and a condensation reaction of two hydroxy groups. As all the reactions up to now are equilibrium reactions, starting conditions as concentrations of silica, source and type, water and alcohols play an important role in the results of gel formation.

From Condensation over Particles to Gel Formation:

It is to emphasize that all prior discussed reactions as hydrolysis and condensation run in parallel, and so a clear distinction in terms of reaction steps is mostly done in stages where certain reaction types are dominant. The already discussed condensation reactions are the basis not only for dimers and oligomers, they are responsible for particle formation, agglomeration to networks, gelation and finally for ageing, too. A distinction is mainly made by the type of reactants. A first example are monomers or dimers that form oligomers in early stages where no larger structures as particles or networks exist. This oligomers tend to grow to particles of a certain size depending on conditions as pH or presence and concentrations of salts in the solvent. The main reason for this is the electrostatic repulsion of negatively charged silica particles and networks. The charges originate from pH dependent hydroxy groups with an isoelectric point at pH 2. Above pH 2 we have negatively charged surfaces that reduce particle approach and fusion if no shielding ions are present. Under these conditions particle formation and growth are favoured. At this stage smaller particles shrink and dissolve in favour of the growth of larger particles due to Ostwald ripening. If charges are shielded by ions or pH is in the acidic region, particle fusions to networks and network fusions in later states is more favourable. This leads to larger particles at basic conditions of pH 7 – 10. At pH 2 – 7 or at the presence of salts favoured particle agglomeration leads to three dimensional

networks and finally gels consisting of smaller particles.

Ageing of Silica Structures:

The same process of Ostwald ripening that favoured bigger particles, is also responsible for ageing in three dimensional gel networks. Solubility of silica is bigger when the curvature of the particle to solve is higher. This results in transport of silica from regions of high curvature to regions of smaller or even negative curvature. For a highly branched network as silica gel this means a strengthening of the small and brittle contact sites of the spheres. Another effect of ageing is the disappearance of smaller pores that are also filled through this silica transport. It is to note that silica solubility in the solvent plays a major role for ageing. Though ageing is not necessary for gel formation, it influences pore size and stability as well as shape in a strong way.

Drying:

Alcogels and hydrogels generally consist of a solid network phase and a surrounding liquid phase. In order to produce aerogels one has to remove the liquid phase somehow without shrinking or densifying the material too much. If an alcogel or hydrogel is exposed to the atmosphere, especially at higher temperatures, the liquid phase evaporates. Due to the porous structure of these gels the evaporation of the liquid phase cannot occur in all regions of the gel at the same time. In fact, evaporation of the liquid part of the gel starts on the surface. The rate of evaporation on the surface of the gel is constant and near the rate of the bulk liquid. As the solvent flows from inside the gel to the surface and the solid part of the gel is not strong enough to withstand the upcoming capillaric and osmotic forces, the gel

shrinks until a critical point is reached, where the structure is rigid enough to withstand these forces and so further shrinkage. At this point the evaporation rate drops the first time as menisci go into the gel and the liquid is transported to the surface. At this stage permeability of the gel is an important factor for liquid transportation. If permeability is low, the conditions inside the gel are not uniform, thus adding additional stress to the drying gel. This could lead to cracks in the gel that in extreme cases even crush the gel to a fine powder. Problems of liquid transport can be influenced by using mixtures of solvents as liquid gel phase. This is the case if one type of molecule in the solvent is more volatile and the out flux of this molecule is compensated by the influx of the other solvent parts. However, if the transport cannot cope with the evaporation on the surface any more, the liquid begins to evaporate inside the gel. This point occurs with a drop in the evaporation rate of the liquid and is considered as another stage during conventional drying. In this stage the adsorption properties of the liquid on the gel are the dominant effects that control the evaporation.

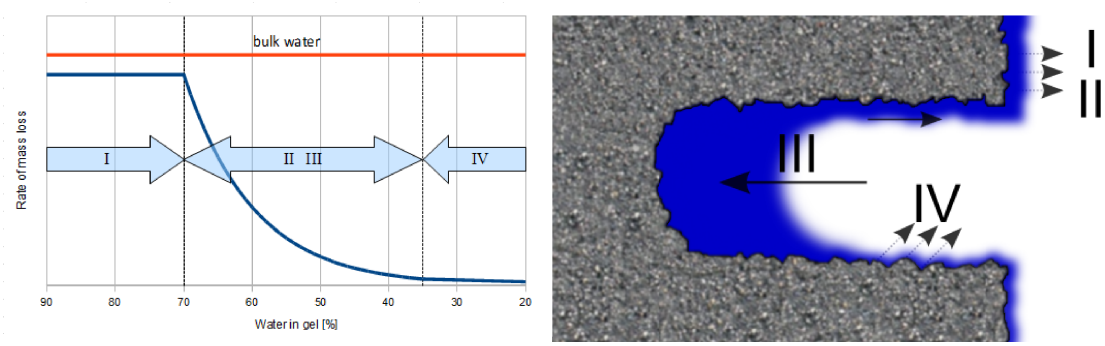

Figures 9a and b: These diagrams show the evaporation of water from hydrogels. Phase I is dominated by the evaporation from the gel surface. Phase II has an additional transport of liquid from the inside of the gel resulting in shrinkage. Phase III shows occurrence of menisci in the gel pores when shrinkage stops. Phase IV shows evaporation of solvent inside the pores when transport to the gel surface lowers.

Note that evaporation sites are important as through evaporation also a drop in temperature takes place that further induces inhomogeneous stress in the gel. First the temperature drops on the surface of the gel and later when evaporation takes place inside the gel, the temperature on the surface is back to ambient conditions again. This shockwave wandering from the surface to the center through the gel may result in cracks and fissures. In order to prevent the gel from shrinking and cracks, it was tried to soften these effects by using additives drying only thin layers of aerogel or by completely avoiding phase boundaries. The phase boundaries that cause this effects can be avoided by either freeze drying or supercritical drying.

Freeze Drying:

One way of avoiding a deforming liquid phase boundary is to freeze the gel and remove the former liquid phase through sublimation. In this case the now solid material is directly removed to the gas phase giving no room to capillaric forces or liquid transport and other forms of stress. But in order to freeze one has to cross the

liquid-solid phase boundary.

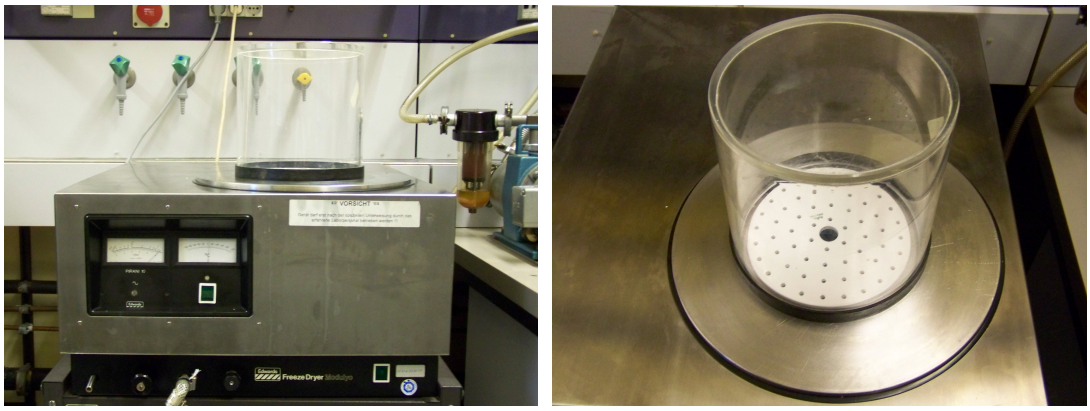

Figures 10a and b: Freeze drying device and freeze drying chamber.

Other effects of freezing are the formation of ice crystals in samples that can further destroy the gel. In fact it is a real problem to freeze the whole gel homogenously without producing ice crystals in the liquid phase. Especially as the gels are known to give room to crystals that destroy the gel structure in the area where the crystals grow. Thus freeze dried aerogels contain at least cracks making them brittle and opaque and in the worst case result in a powder of aerogel that has nothing in common with its original shape. As measurements will show, the structure and especially the pores of the gel are also influenced by means of freeze drying.

Supercritical Drying:

Another way of avoiding the stress of capillaric and osmotic forces in gels through getting rid of a phase boundary transition is to use supercritical drying. This way follows a special pathway through the supercritical region in the temperature – pressure diagram of the solvent used for drying. For this process the pathway starts in the liquid phase where temperature is raised above the critical point of the solvent.

The pressure is then also raised above the critical point. At this point in the supercritical region there is no phase boundary between liquid and gas phase. The pressure can be lowered keeping the temperature constant. Finally the temperature can now be lowered as discussed for the gas phase, thus avoiding phase boundaries and the forces that could cause shrinking or cracks in the gel.

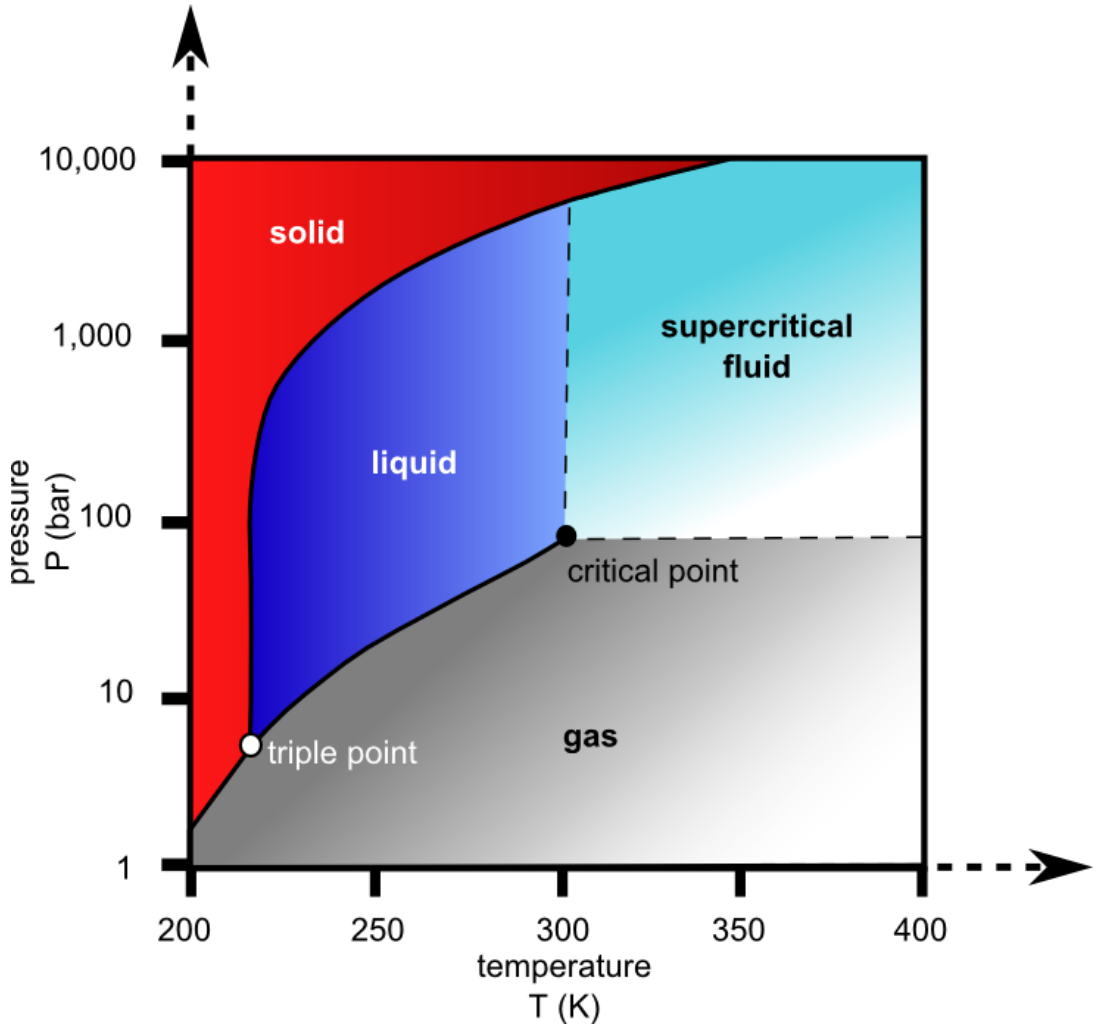

Figure 11: Phase diagram of carbon dioxide.

Table 1: Supercritical conditions for various substances. Taken from the book Sol-Gel-Science (page 502).[1]

Substance	Formula	T_C [°C]	P_C [MPa]
Carbon Dioxide	CO_2	31,1	7.36
Freon 116	CF_3CF_3	19,7	2.97
Methanol	CH_3OH	240	7.93
Ethanol	CH_3CH_2OH	243	6.36
Water	H_2O	374	22

The solvent chosen for supercritical drying is very important, not only for appropriate temperature and pressure values of the liquid it also has either been used in gel formation or it has to be exchanged for the present liquid in the gel. Of course hydrogels can be dried by going above the critical point for water but normally one would like to use milder and technically less demanding pressure and temperature ranges. So in supercritical drying solvents such as ethanol or carbon dioxide are employed. In case of gels based on silica alcoxides supercritical drying with ethanol or methanol is an option that reduces the demand for liquid exchange. Supercritical drying with carbon dioxide has become common through its widespread use as extraction media in food industry. Its usability for food and medicine is, however, not its only advantage beside its commercially availability. The main reason of its use is probable the mild drying conditions of about 32 °C and 74 bars. As it is at least not practical to prepare gels in liquid carbon dioxide, due to the high pressure needed, it is necessary to change the liquid from the gel to other solvents. As water is not miscible with carbon dioxide and considerable amounts of water can cause cracks during drying, a direct exchange of carbon dioxide for water is out of question. For that reason one has to use an additional intermediate solvent and so two solvent exchanges are necessary. For that purpose acetonitrile and acetone are good

candidates for their miscibility with water and carbon dioxide. If one has to do solvent exchange, one can also benefit from it. So as acetone has been known to reduce drying times and prevent shrinking and cracking conditions and due to its low price and readily availability, it is commonly used.

The solvent exchange can simply be done by bringing the gel in another solvent. Exchange times can be estimated by use of solvents with a higher density. Under this conditions the gel first floats on top of the solvent until most of the solvent is exchanged and the gel block sinks to the bottom due to the higher density. As geometry and size of the gel block play obviously an important role, permeability of the solvents inside the gel is important, too. Therefore these experiments only gave a rough estimation on solvent exchange times which for the gels in use were in the range of about two hours. This time should of course be extended to an amount where one is sure that at least most of the solvent has been exchanged, even under different and more unfavourable conditions.

A typical drying procedure under supercritical conditions with carbon dioxide in an autoclave is now described, as there are some points that demand special attention. The gel is put in the autoclave immersed in a solvent that is appropriate for drying with supercritical carbon dioxide such as acetonitrile or acetone. The gel has to be submerged in solvent to prevent drying of the gel before the autoclave is closed and under liquid carbon dioxide. As the gel is inside and the autoclave is closed and at its temperature above the critical point, it is slowly put under pressure until liquid carbon dioxide can be added at a pressure of about 45 bars. During pressurising the diffusion of carbon dioxide into the solvent can be watched as an increasing volume

of solvent with slightly different optical properties. As more and more carbon dioxide is dissolved in the solvent, the mixture increases in volume and is, dependent on the volume of the autoclave and the amount of solvent used, likely to fill the autoclave. During this initial step of filling the autoclave, the rise in pressure is slow until no gas is left inside. Another region of slow pressure rise is close the critical point. Once beyond the critical point the pressure rises fast and the solvent mixture can be exchanged for supercritical carbon dioxide. It is to note that the influx of carbon dioxide as the out flux of the mixture should be balanced in order to avoid harsh pressure changes. It is further to note that the flux in the autoclave volume should be uniform for the gels to have similar drying times. It is important that the flux is not too high to prevent cracking of the gel. In general, it is important not to change conditions abruptly which could also lead to cracks in the aerogel. After some time drying the gel and the solvent mixture has been replaced by supercritical drying, especially after no solvent can be detected at the outlet of the autoclave, it is time to close the influx valve and slowly de-pressurise the autoclave. Finally under environmental pressure again the aerogel can be removed from the autoclave. Depending on the manufacturing conditions and the properties of the gel, it is likely to be transparent. It is to note that marking certain blocks of gel for drying is problematic and should be done by putting the gel in distinguishable open cases that do not disturb the liquid flow and withstand carbon dioxide. It is further to note that putting other substances that are immiscible with carbon dioxide or react with any part as gel or solvents used is likely to influence drying resulting in opaque gels, cracking or shrinking.

The method of supercritical drying avoids any phase boundaries, has mild drying

conditions and can even be used in synthesis of aerogels usable in food industry or medicine. However this comes at costs as necessary high pressure treatment and special equipment like an autoclave. Up to now this method is the only one that can be widely used and provides high quality bulk aerogel of sizes that are only limited by the load volume of the autoclave in use. These are the reasons why supercritical drying with carbon dioxide as medium is the main drying method used in this work.

Building the Autoclave:

As supercritical drying is the method of drying applied during this work and available autoclaves were not up to the task, it was necessary to build one that can handle the special needs during supercritical drying with carbon dioxide and provides sufficient space for loading a batch of gels for drying. One property that is especially important that other autoclaves available at the laboratory did not provide are gaskets that withstand supercritical carbon dioxide for periods of several days. Despite of easy handling most rubber gaskets are mostly not up to the task and start leaking after several hours of use. While this is not a concern for measurements and short time use these were not suited for drying. In contrast, gaskets made of Teflon are stable under the conditions of supercritical carbon dioxide. Concerns regarding instability of Teflon gaskets at elevated temperatures do not apply at drying conditions of supercritical carbon dioxide that doesn't need to surpass 40°C. However for long term and standard connections metal gaskets seem to be the best choice. Metal gaskets withstand supercritical carbon dioxide easily and endure a wide temperature range. The most important feature is that in contrast to Teflon metal gaskets are, if at all, much less deformed during use. This shape stability ensures re-usability of these gaskets over a long time. Supercritical carbon dioxide can be identified as an inhomogeneous looking phase with streaks. Other visible effects are the increasing carbon dioxide concentration in the solvent to exchange and its phase boundary. In order to see these phenomena and thus to gain better control over the drying process, it is good to have windows in the autoclave. As the drying process requires the supercritical phase of carbon dioxide, it is necessary to

thermostate the autoclave to about 40°C and it has to sustain at least 100 bars of pressure. Both values of temperature and pressure are calculated to be higher than necessary in order to have a security range. An additional security range is advised as an autoclave should not be run at its limits. An important point in drying bulk gel samples in an autoclave is the flow of solvent in the autoclave. In order to have even drying times and conditions the flow in the autoclave should be homogeneous. Otherwise drying times are increased or gels that are positioned in higher flow areas could crack. To ensure a homogeneous flow the autoclave was constructed with 3 connected inlets and two connected outlets.

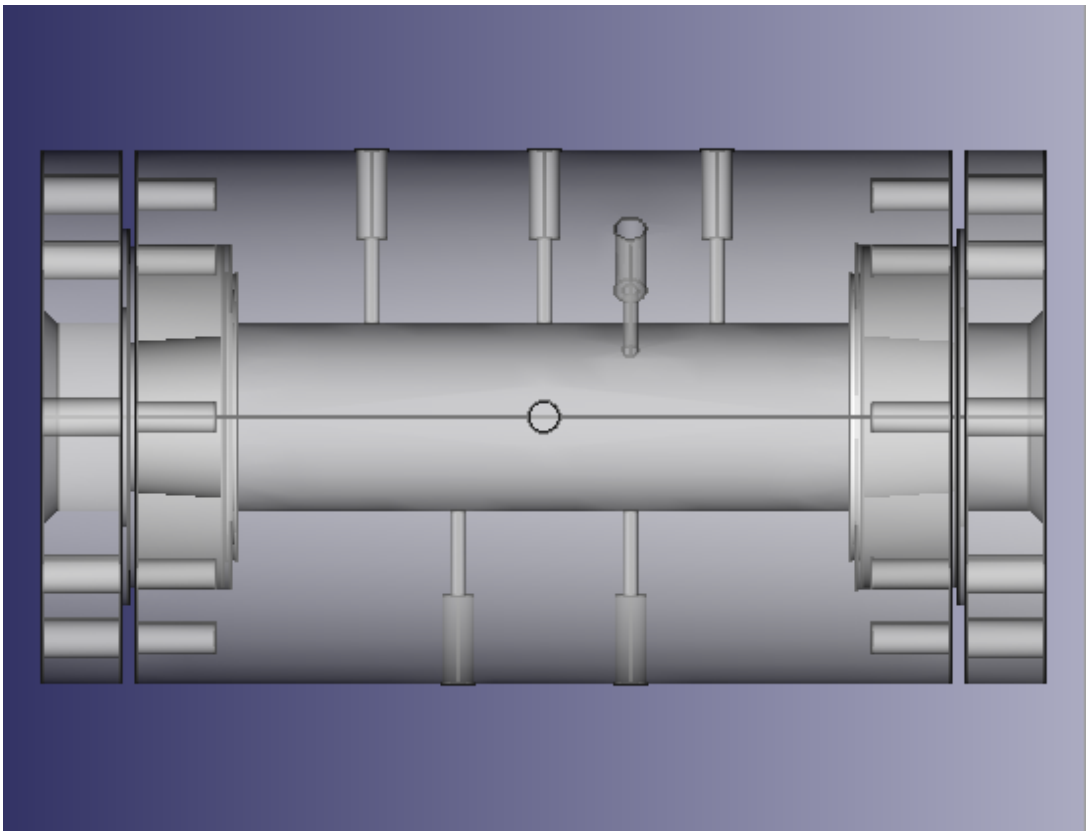

Figure 12: Showing the assembled autoclave with teflon gaskets, windows and flanges in a side view.

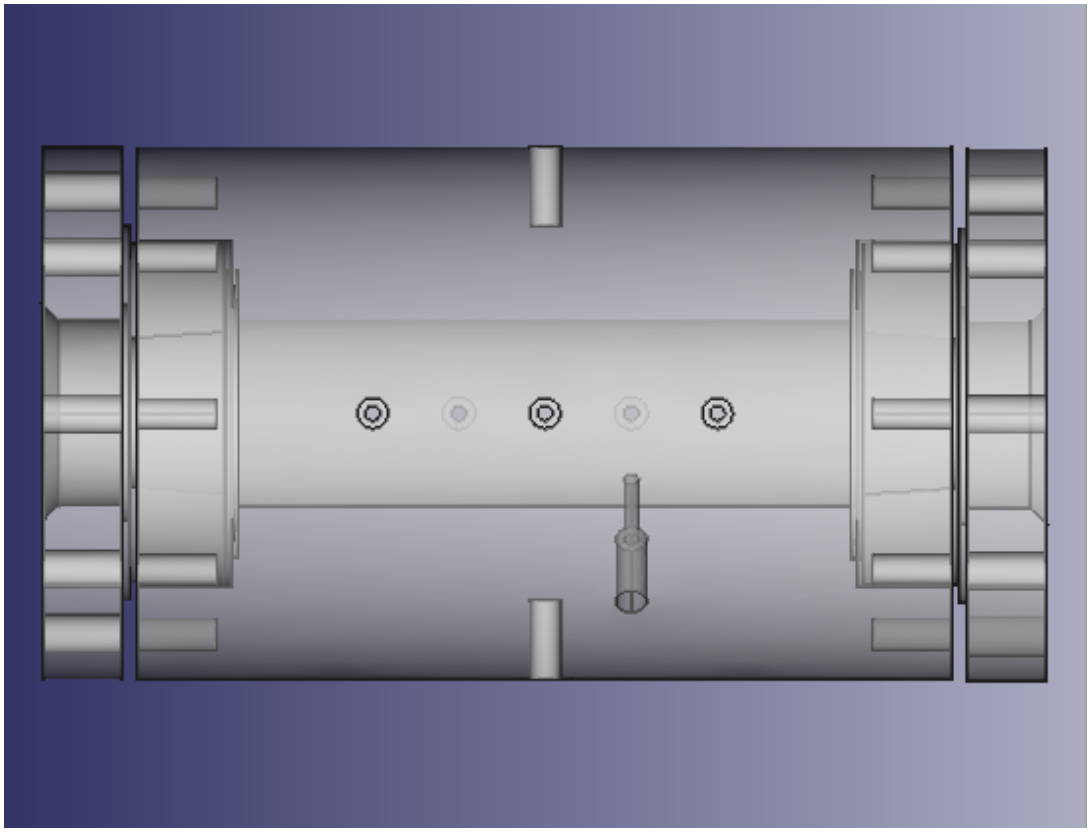

Figure 13: Showing the assembled autoclave with teflon gaskets, windows and flanges from the top.

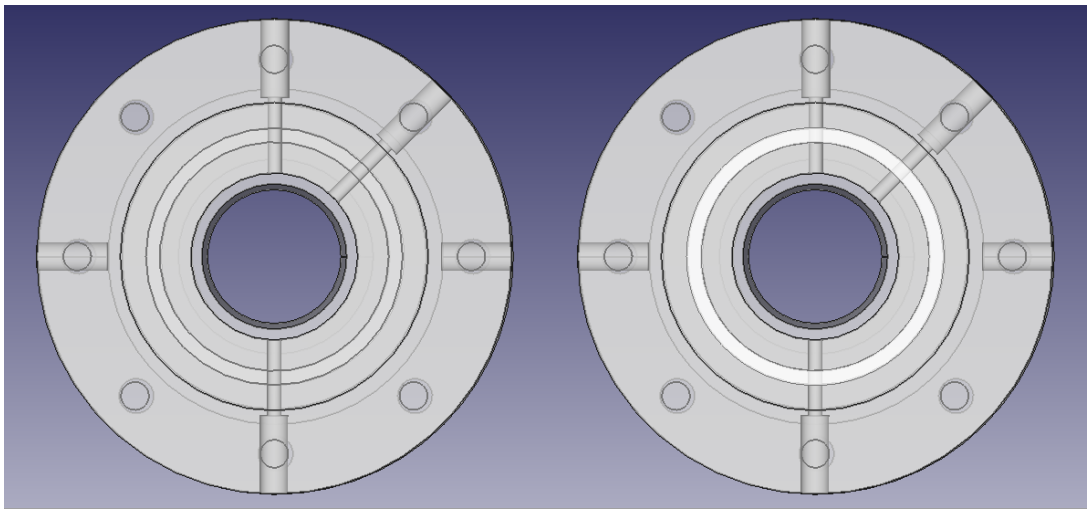

Figures 14a and b: Showing the front view of the autoclave without and with teflon gasket.

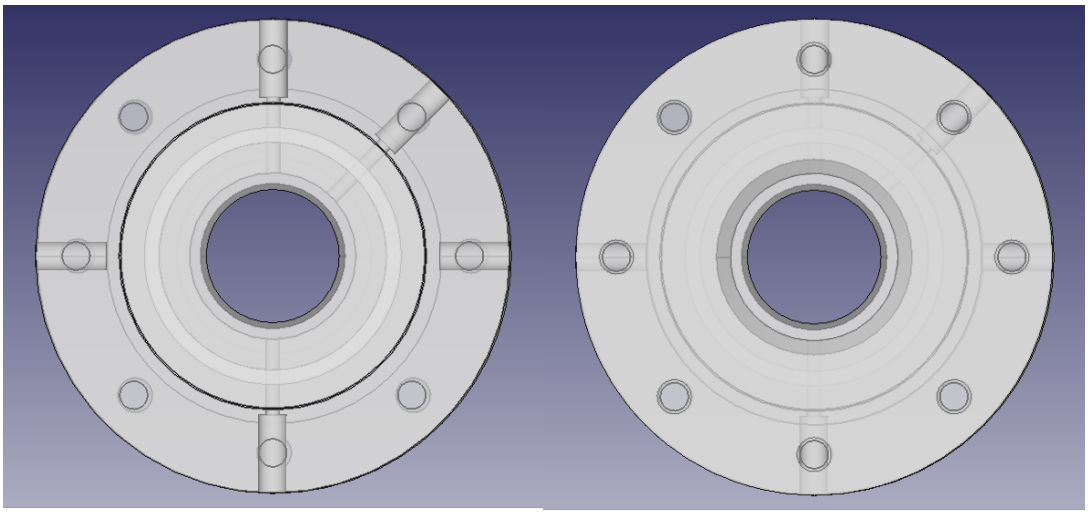

Figures 15a and b: Showing the autoclave in front view with teflon gasket and window. Same view with the flange on top of the window.

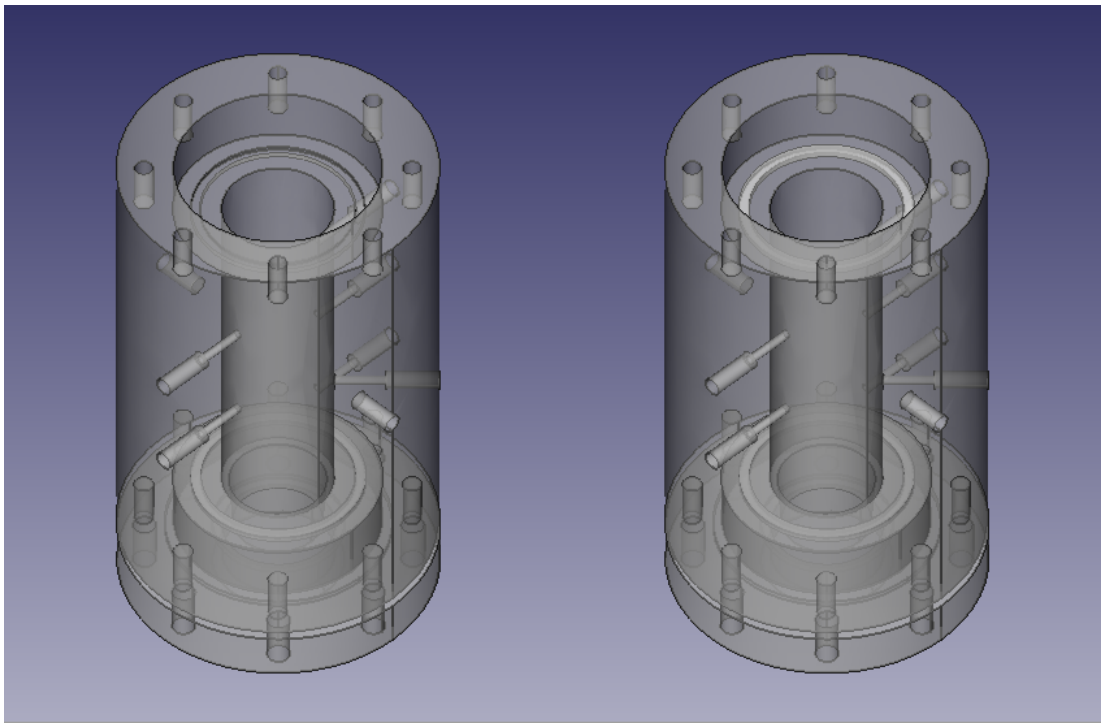

Figures 16a and b: Isometric view of the autoclave without and with teflon gasket.

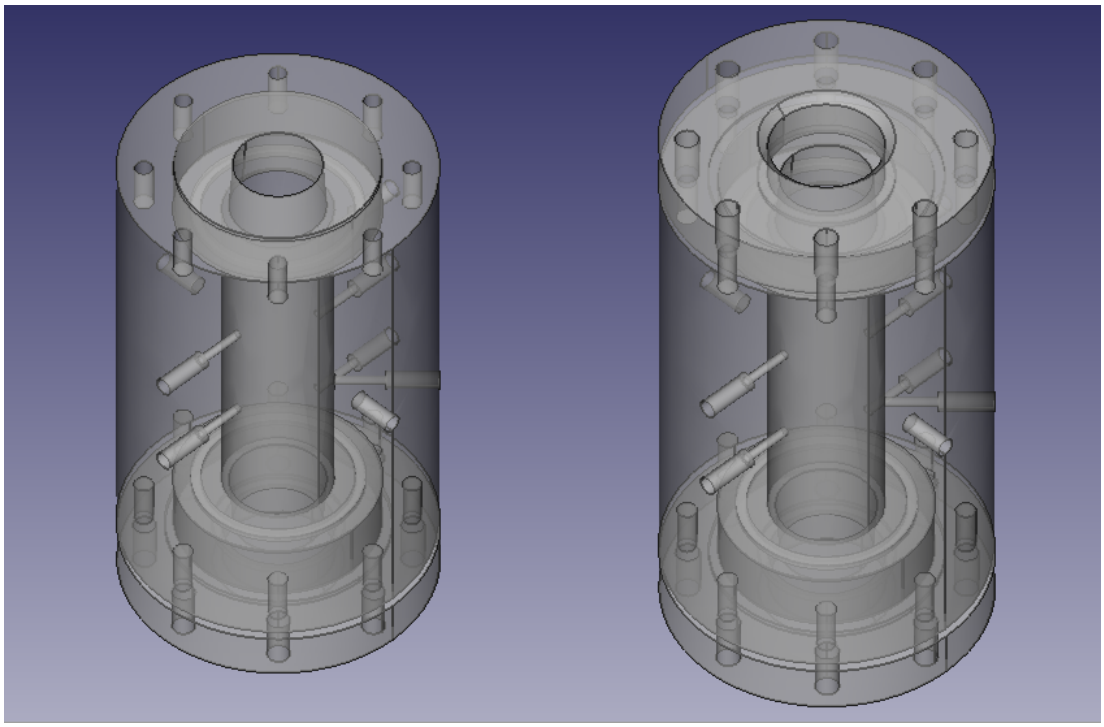

Figures 17a and b: Isometric view of the autoclave with window and with window and flange on top of the Teflon gasket.

As liquid carbon dioxide is used for drying, a HPLC pump is sufficient to generate the flow in the autoclave. Of course a gauge for pressure control is necessary as a security valve. As the outlet valve is open for most of the drying process it has to be heated to prevent freezing due to constant evaporation and gas expansion at the valve. The original blueprints for the autoclave were provided by Prof. Smirnova from the high pressure research centre at Erlangen. The material for the autoclave is V4A steel and was delivered as cylindrical block. This block was processed in the workshops at the university of Regensburg. The steel cylinder was cut to its designated size. The hold volume of the autoclave was drilled out of the main block. The fittings of the autoclave and an appropriate security valve were ordered from Swagelock. Several parts as pipes, pressure gauges, pumps and valves were already

present and were used in assembling the device. The thermostat consists of a heating tape around the autoclave and a controlling device with a thermometer which is mounted inside the autoclave. For the fittings metal gaskets were used and for the main access points the windows of the autoclave teflon gaskets were used because of their size.

Autoclave Operation Instructions:

More important than the description of manufacturing the autoclave is how it is used in the process of supercritical drying. This seems especially important as there are some common pitfalls one comes across when first using such devices. As many good instruction manuals we start with the important parts of the drying device as they are encountered following the carbon dioxide flow depicted in figure 18.

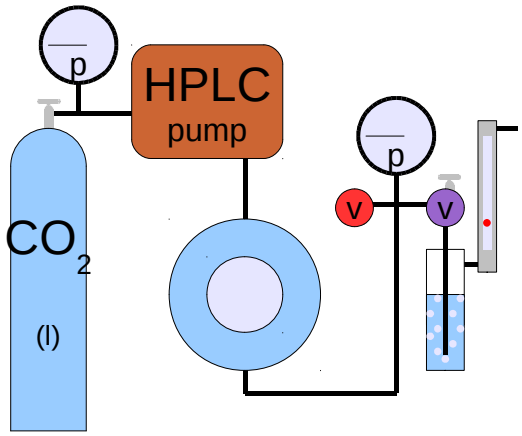

Figure 18: Showing the important parts of the supercritical drying device concerning the carbon dioxide flow.

On the beginning of the carbon dioxide flow is the carbon dioxide source in the form of a bottle of liquid carbon dioxide with a riser. This bottle is connected via a pressure gauge (Figure 19a) with a high pressure liquid chromatography pump (Figure 19b).

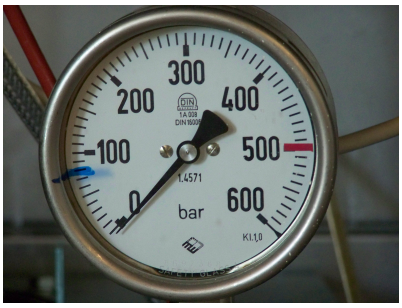

Figures 19a and b: One of the analog pressure gauges. Digital ones where used additionally. A cooled high pressure liquid chromatography (HPLC) pump from Gilson was used for drying.

The pump provides the necessary pressure as the carbon dioxide source typically provides pressures around 50 bars. The carbon dioxide flow then enters the autoclave where the drying takes place. From there the flow of carbon dioxide reaches another pressure gauge with a security valve and an outlet valve. It is to note that due to permanent gas expansion and evaporation the outlet valves have to be heated in order to prevent freezing of the valve. Special care has to be taken that in case of emergency the security valve will remain intact, so it is heated, too. The outlet valve leads to a washing flask and finally to a flow meter before it is released to the air or in our case to an exhaust hood. Not depicted in figure 18 is a thermometer inside and a heating tape around the autoclave as well as the necessary heat controlling unit. For the thermometer and heat control see the figures 20a and b.

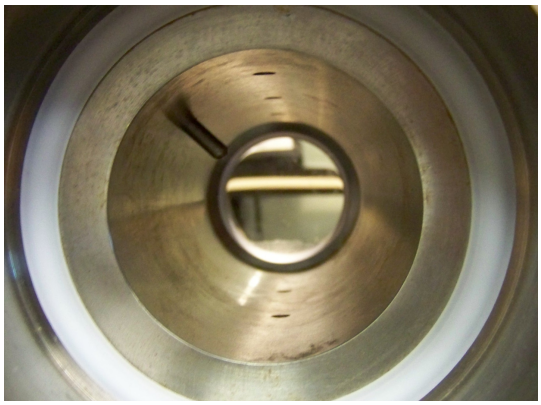

Figures 20a and b: Inside of the autoclave with the thermometer rod in the upper left. Heat control unit.

The drying process typically starts by loading the autoclave that is partly filled with a solvent suitable for the gels as well as carbon dioxide. As already mentioned water should be avoided as it may may remain in the gel and can cause cracks or fissures in the aerogel or leads to shrinkage. Acetone or acetonitrile are suitable solvents for normal alcogels. It is important that the gels should have contact to the solvent in order to avoid evaporation and drying before the gels are under supercritical carbon dioxide. As the autoclave is loaded it has to be closed and brought to a horizontal position to provide an even flow inside the autoclave. Now the valve of the carbon dioxide source can be opened slowly to set the pipes under pressure. During this step it is possible that some of the carbon dioxide breaks through the HPLC pump into the autoclave and rising the pressure there slowly. As long as the pressure before the HPLC pump is much higher than inside the autoclave the pipes may freeze due to the evaporation of liquid carbon dioxide. So if the pipes get cold and the pressure in the autoclave is not rising despite of the running HPLC pump the pipes should be heated with a heat gun. When the HPLC pump is switched on, it is important to ensure proper cooling of the pump if this is required for that model. As we have changes in

the autoclave we have two pressure plateaus. One when the autoclave is slowly filled with liquid carbon dioxide. And another one for transition between the liquid and supercritical state of carbon dioxide. In order to speed up the drying without the risk of ruining the gel it is best to start heating the autoclave to 40°C when it is filled with carbon dioxide. When the pressure rises over 90 bars, the outlet valve can slightly be opened to ensure an equal influx and outflux of material from the autoclave. It is to note that if the autoclave has observation windows it is possible to better control the process and see the filling of the autoclave. It is further to note that with this method it is possible to observe the increasing mixture of the solvent with carbon dioxide. Even supercritical dioxide can be observed by visible streaks in its phase. The drying is complete if no more solvent leaves the autoclave with the carbon dioxide flow. When the drying is complete the valve of the carbon dioxide source should be closed followed by switching off the HPLC pump. As the pressure in the autoclave slowly falls, the same pressure plateaus are achieved. Sometimes when the pressure fall stops, the outlet valve has to be opened a little more for de-pressurise to continue. When room pressure is reached, the autoclave can be opened and the aerogels can be removed. Finally the heating is switched off together with the remaining devices such as thermostats for cooling the pump or additional pressure meters.

Influencing Silica Growth:

Approach in Natural Systems:

When starting to think of how one could influence or direct the growth of amorphous silica in order to get possible useful structures, the first look will probably aim at how living nature makes use of amorphous silica. As we all should have recognized biomineralisation is in common use among life forms in this biosphere. There are several forms of biomineralisation. Such forms include simple precipitation of inorganic material, controlled oxidation reactions and directed growth of inorganic substances to form composites. The most interesting and sophisticated method of these is of course the directed growth to form highly adapted and enhanced composites designed to fit their tasks like bones that have a flexible organic part that is resistant to pulling forces and an inorganic part that is resistant to pushing forces. The most known example is most probably that of calcium carbonate in the form of shells. Just like calcium which is more or less omnipresent in the biosphere silica is also very common dissolved in water and one abundant source to many forms of life. Life forms managed to control growth of silica to enhance and strengthen their structures. The easiest form however is to just include silica in the structural parts to enhance stability like in bamboo. A more sophisticated way of use is to control the growth of amorphous silica to form complex structures such as valves which can be observed in diatoms. Diatoms not only build their complex parts out of amorphous silica, most of their structural shell in the cell walls is made of silica that is grown by the diatoms themselves.[13] It has been shown that this is done by altering local concentrations of silica precursors through active transport and by providing

structured templating organic peptides. Some of these templates consist of lysine rich peptides containing repeating amine groups in regular distances that encourage the growth of silica nano spheres along the template. This type of directed growth has been proven by extracting these organic templates and forming new silica structures in a silicic solution with these templates. Fine silica structures in nature are finally protected from dissolution by an organic coating.

This interference with silica growth has also been done by synthesizing amine or polycationic groups in polymers. These polymers have been shown to influence the growth of amorphous silica by acting as a template structure where amorphous silica can grow to certain shapes such as columns or spheres.[14] It was also observed that polyethyleneglycol accelerates reaction times for amorphous silica resulting in decreased gelation times.

Another method of influencing silica growth is the occupation of certain surfaces on a crystal which also influences crystal growth of silica crystals to provide different shapes, such as “rope”, “toroid”, “discoid”, “pinwheel”, “wheel”, “gyroid”, “bagel”, “shell”, “knot”, “clock” or “eccentric” shapes.[15] The growth on the surface of crystals is hindered on occupied surfaces and so influences growth and shape of the crystals. For the present work of controlling growth of gels and aerogels this approach cannot be made as there are simply no crystals and therefore no such surfaces. Another point against this approach is that dense materials like crystals are in contradiction to the construction of lightweight aerogels with their per definition low density, which are the aim of this work.

There are of course other ways of influencing formation of amorphous silica that occur in nature which are not part of the living realm as previously mentioned. There is the possibility of a combination of crystals and amorphous silica with growth directing methods as found in biomorphs. Biomorphs are substances where for example carbonates of barium or calcium or better their crystals are covered by amorphous silica and grow according to the present environmental parameters such as pH or additives in homoeopathic concentrations to many shapes such as “helices”, “worm like structures”, “sheets”, “raspberries” or “dumbbells”.[16–19] Unfortunately these structures are also dense and are only embedded in amorphous silica so it is like embedding biomorphs into an amorphous silica gel or aerogel. Indeed gels where used as a reaction media for the synthesis of biomorphs, but are dissolved after synthesis. For the control of growth in gels this methods are therefore not well suited.

Surface Active Substances

The use of surfactants to form biomorphs or crystal like shapes structures can be an approach for influences on gels, too. Therefore, I investigated the influence of surfactants on gel formation. As mentioned in the chapter of gel synthesis the presence of salts helps shielding the negative charge of growing amorphous silica particles, so it is a good assumption that cationic surfactants influence the growth of gels. Common cationic surfactants are trimethylammonium head groups with an alkyl chain. In order to limit the influence on the added surfactant, I decided to use chloride as the surfactant counter ion, because chlorides were already present in the reaction medium from hydrochloric acid. In applying this approach additional different salt combinations are avoided. I used different alkyl chain lengths and concentrations to influence the aerogel structure. There is indeed an effect on the gel

formation that is unfortunately not reproducible. The effect takes place with different lengths of alkyl chains and results in more or less ordered patterns of holes in the gel structure (Figures 21).

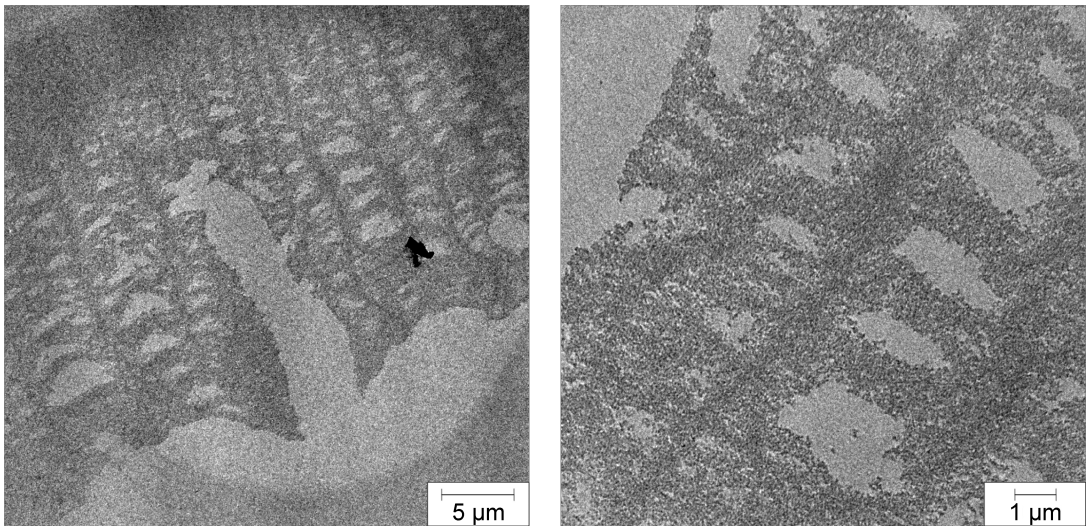

Figures 21: Not reproduceable ordered patterns of holes in silica aerogel.

As these cationic surfactants seem to influence the gel formation process but in a not reproducible way, I assume additional conditions are necessary and that the effect might be based on foam present during the gel building stage. Therefore I tried to switch to cationic surfactants with a higher tendency of self assembling to form template structures. This should provide an easier recognition of changes in the new formed modified aerogels in comparison to the untemplated references. In addition to self assembly, I tried to introduce chirality into the aerogel. This should further provide proof of changing the structure of a normally amorphous achiral silica aerogel.

Recently it has been shown that chirality can be introduced into xerogels with the

help of chiral surfactants.[20,21] Besides several advantages, xerogels have some disadvantages. They shrink during the drying process, which results in a dense and rigid material. By contrast, aerogels retain their size during drying,[1] which leads to a very low density material with unique properties, such as low weight with good thermal isolation, high porosity, and a large surface area, making them interesting, for example, for catalysis and adsorption processes.

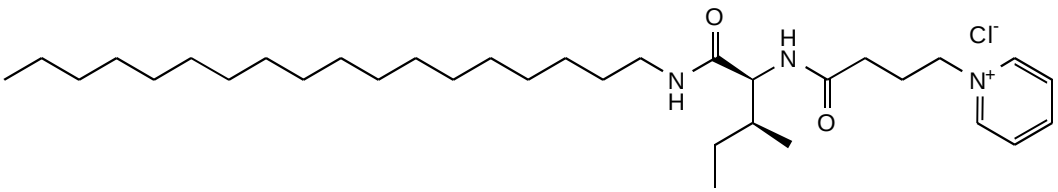

Figure 22: Structure of the compound L-4PyCl.

As chiral template we use the surface active compound L-4PyCl (Figure 22), which has already been used as template for chiral xerogels.[21]

Synthesis of the Surfactant

The synthesis of the surfactant has already been shown in literature.[20–22] The z-protected amino acid L-isoleucine (purum. Fluka) was coupled with octadecylamine (puriss. Fluka) employing the peptide coupling reagent N,N'-dicyclohexylcarbodiimide (DCC). The amino acid was dissolved in ethyl-acetate at 0°C. DCC was added and stirred for a hour. Ocatadecylamine was added and the solution was stirred for another hour at 0°C. The cooling bath was removed and the solution stirred over night. The temperature was risen to 45°C and another 10 hours of stirring followed. Side-products were filtered off at about 45°C. The product

was filtered off afterwards at room temperature.

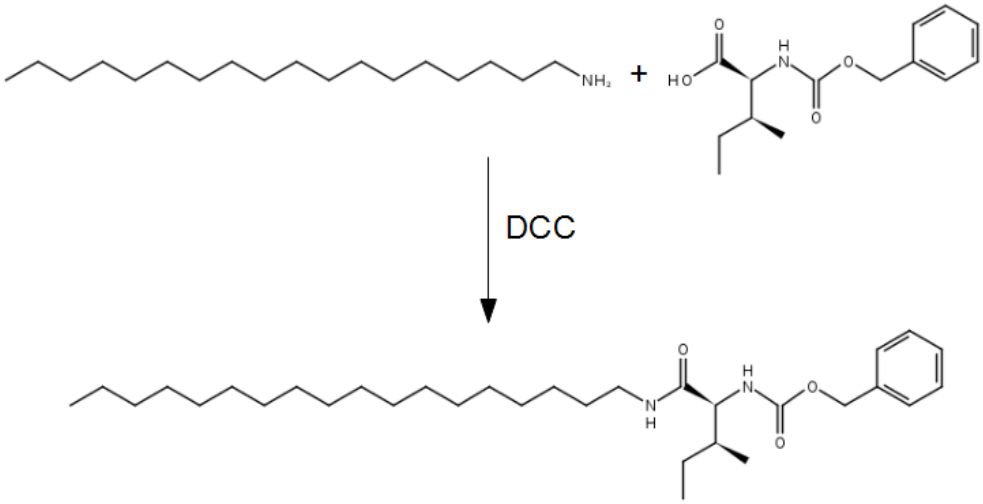

Figure 23: Reaction scheme of step I.

The z-group was removed with platinum as catalyst at 10 bars on activated charcoal under hydrogen. The catalyst on charcoal has been removed by filtration.

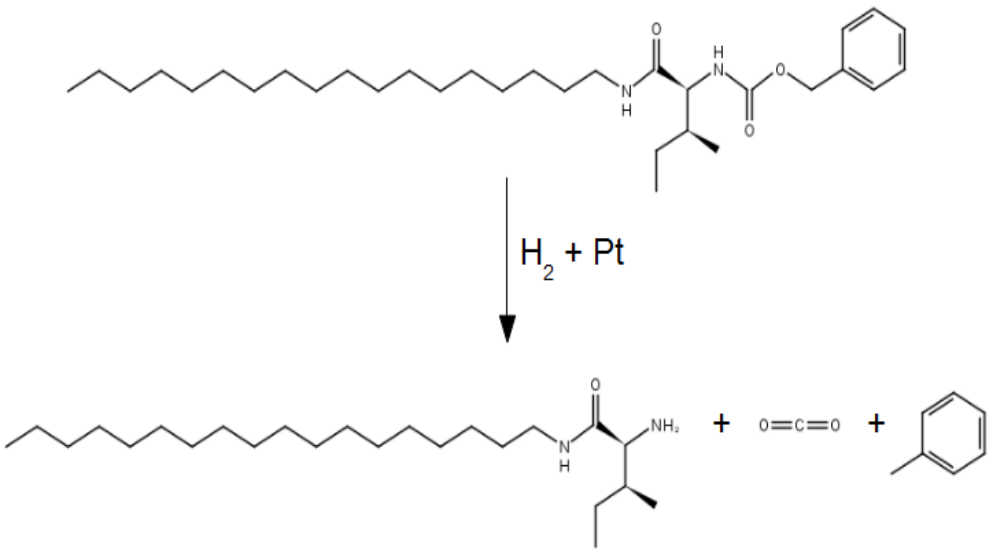

Figure 24: Reaction scheme of step II.

The unprotected amino acid was then coupled to 4-chlorobutyryl chloride. The product of step 2 was dissolved in Tetrahydrofuran (THF). At 0°C Triethylamine was added and finally 4-chlorobutyryl chloride was added and stirred for an hour. After solvent removal the product was used in the next step.

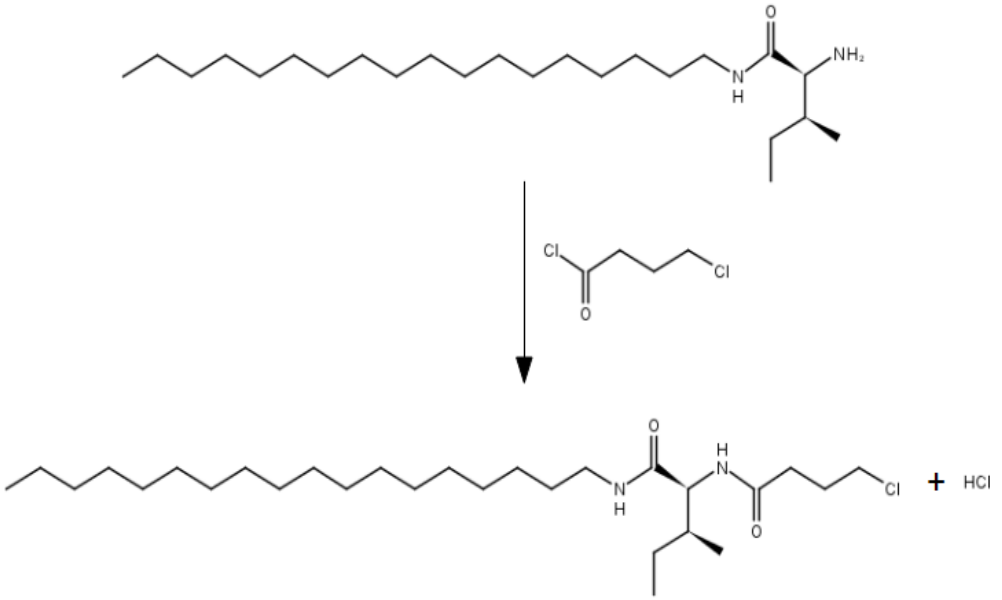

Figure 25: Reaction scheme of step III.

Finally, the surfactant was obtained through reflux in pyridine (99% Acros Organics) under nitrogen atmosphere. After solvent removal the product was purified twice via recristallisation in methanol-ether mixtures. The purified product is a light white powder and the NMR spectra of the product were compared to literature.

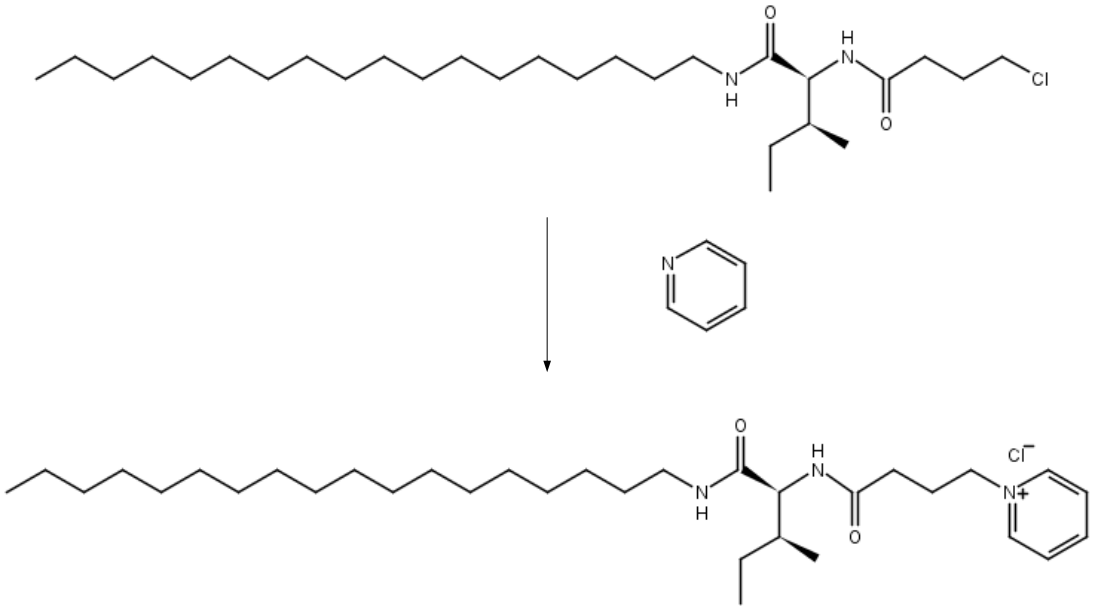

Figure 26: Reaction scheme of step IV.

Gel Forming

A typical procedure for gel formation was as following.

For the formation of the gels the surfactant was dissolved in a mixture of 2.74 ml of 11.3 wt% of aqueous ammonia solution and 1.17 ml of ethanol (absolute J.T.Baker). This mixture was cooled in an ice-bath, where 0.085 ml of tetraethoxy orthosilicate (TEOS) (for Synthesis, Merck) was added.

Drying

The aging and drying processes were specially optimised in order to obtain aerogels instead of xerogels. Ageing was performed at room temperature overnight, followed by solvent exchange with acetone in several steps. The gels were then dried with CO_2 under supercritical conditions at 40°C and a pressure above 90 bars under constant CO_2 flow. The drying time depends on the solubility of the gels' liquid phase in

supercritical CO_2 and the amount of solvent, which needs to be removed. All the gels were dried until no acetone could be detected at the autoclave outlet. The minimum drying time was one day.

Heat Treatment

In order to remove the residues of the organic templates the aerogel was heated for several days at elevated temperatures. In order to quantify the temperature and time needed to remove the organic remains without modifying the aerogel surface too much, a thermogravimetric analysis of a templated aerogel was done (see figure 27).

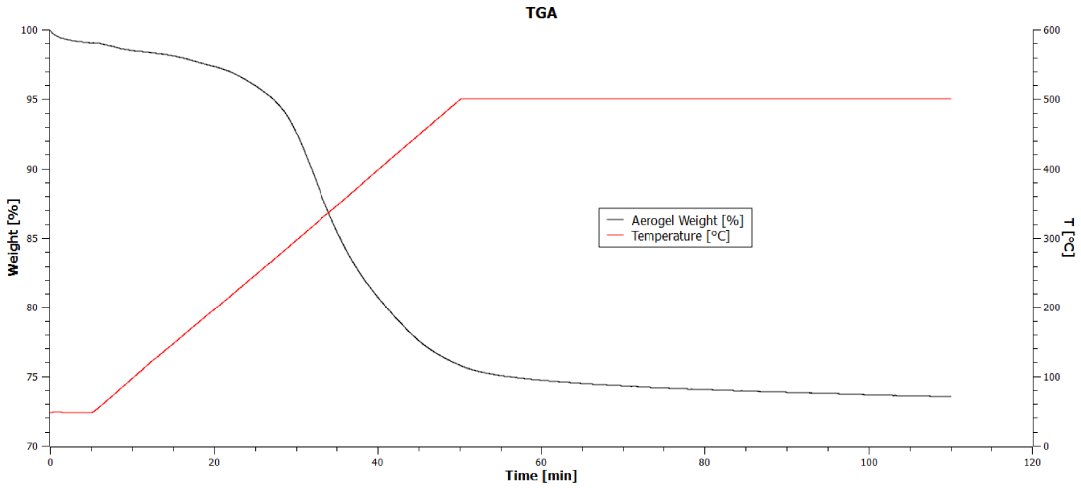

Figure 27: TGA of aerogel with organic remains from the template.

Based on these results some of the samples containing surfactants were heated to 350°C for 5 days in air after drying in order to remove the organic material.

Analysis Methods:

Rotational Angle Measurement:

Chiral substances are known for their influence on linear polarized light. For example a solution of a chiral substance alter the angle of linear polarized in an reproducable direction and dependent on the concentration the rotational angle is also specific for a certain sample material. A device for measurement of rotational angles typically consists of a light source, two linear polarisers, and a detector. The sample is put between the two parallel polarisers and one polariser is rotated to the angle where the most light shines through to the detector. At last the rotational angle is read out. In principle it is also possible to measure the rotational angle of certain wavelengths.

Aerogels as Rotational Angle Measurement Samples:

The biggest problem with measuring aerogels is the fact that we have a solid instead of a solution. Having a heterogeneous solid system the problems of measurements are obvious. The angle between the polarisers is strongly dependent on the path of the light through the aerogel. This reduces reproducibility of measurements to an unbearable extent. Therefore the measurements can give only a hint on if there is chirality or not. Another problem of this method are the different optical properties as for example some modified aerogels are no longer transparent but show opaque colours and light scattering effects that prohibit most aerogels from being reliably measured by this method.

CD-Spectroscopy:

CD -Spectroscopy is based on absorption of circular polarized light. In circular polarized light the magnetic and electric field maintain their magnitude and rotate perpendicular to each other and the propagation direction either clockwise or counter-clockwise. This is in contrast to linear polarized light where the magnitude is changing and the direction of magnetic and electric field stays constant. In fact clockwise and counter-clockwise circular polarized light of the same “strength” is sent through the sample. The resulting spectra give the difference in “strength” of the light after absorption in the sample occurred against the wavelength of the light. The results give only a non zero signal if the investigated material is chiral and light interacting. The ratio of enantiomeres can also be detected if the system is calibrated with a known concentration of one enantiomere. This technique is commonly used today in the form of UV/Vis – CD-Spectra for determining the secondary structure of proteins. It is mainly used for solutions of the sample.

Aerogels as CD-Spectroscopy Samples:

For use with solid aerogel some tests have been made. It is of course not possible to consider bulk aerogel pieces for measurements, because the optical properties of aerogel and modified aerogel can differ significantly as some forms of modified aerogel are opaque in contrast to transparent reference silica aerogel. As already mentioned, the inhomogeneity of solid aerogels is another big problem. In order to overcome inhomogeneity and hardly reproducible thickness of samples, the aerogel is ground to a homogeneous powder and applied to a transparent adhesive tape for measurement. The powder also gives other problems in terms of signal strength as

light is scattered from the sample. Finally the results showed another problem, as the used transparent adhesive tape seems to also give signals in the resulting CD-Spectra. Therefore this technique at least in the used form for solutions seems unusable for direct measurements of chiral properties of modified aerogel.

Gaschromatography:

Gas chromatography is an analytical method for separating and analysing samples. The samples are transferred into gas phase and put in a stream of carrier gas. The gas mixture is sent through a gas chromatography capillary in an oven. According to the adsorption properties of the capillary walls different substances within the samples are hold back inside the capillary for a different retention time. After the gas has passed the capillary its ingredients can be detected in various ways. One way is to measure the heat conducting properties. Another one is to inject the gas into a flame and measure the change in heat. This way mixtures of solutions and gases can be separated according to their properties and detected even in a quantitative way.

Figure 28: Gas chromatograph with auto-sampler and head-space auto-sampler.

Aerogels as GC-Samples:

However aerogels as solids cannot be measured directly this way. The method of gas chromatography was employed to detect if chirally modified aerogels adsorb a part of an racemic mixture resulting in chiral solution. For that purpose a chiral column was used. For these experiments different concentrations of tartaric acid were prepared. To each of that solutions a known amount of chirally modified aerogel was added. After adsorption took place the aerogels were filtered and the remaining solutions were analysed with gas chromatography. Unfortunately the results showed no influence of the aerogels on the racemic solutions of tartaric acid. One explanation of this can be seen when applying methods of electron microscopy to the

chirally modified samples of aerogel. These measurements show chiral helical fibres of about 20nm diameter and several hundred nanometres length. Considering the different size of chirality in the aerogel and in a solution of tartaric acid it seemed as if we put screws in a racemic solution. The chirality has to be on the same scale of size to take an effect on each other so the adsorption of a normal chiral or racemic solution on chirally modified aerogel resulted in no chirality based effects.

BET Measurements:

BET is a method for determining the surface area and estimation of pore sizes in porous materials. BET is named after their inventors: Brunauer Emmet and Teller. With this method the surface area can be measured through adsorption of gas molecules, in most cases nitrogen, onto the former desorbed sample at the temperature of liquid nitrogen. With the known amount of gas added or removed and the pressure in the measurement chamber, it is possible to record adsorption or desorption isotherms. In such a system the surface is proportional to the adsorbed gas in a certain range of pressure resulting in the surface area of the sample. In order to estimate pore sizes, it is necessary to form multilayers of adsorbed gas molecules to subsequently fill the pores and so getting a lower surface of the sample. The actual values of pore sizes measured are dependent on assumptions of pore geometry and empirical formulas resulting in different values for different evaluation methods, thus giving only a hint at the real values. However, changes in modified gels and thus relative measurements should give a good results for interpreting what happens in such modifications, especially concerning surface area or pore sizes.

Figure 29: BET ASAP 2000 from Micromeritics.

Aerogels as BET-Samples:

Aerogels with their low density and high porosity are especially well suited for measurements of this kind. Their thermal stability also offers easier and faster ways for desorption during sample preparation through elevated temperatures up to 150°C. It is to be noted that for its low density and high surface area the sample amount has to be adjusted in order to get good results in a reasonable time frame.

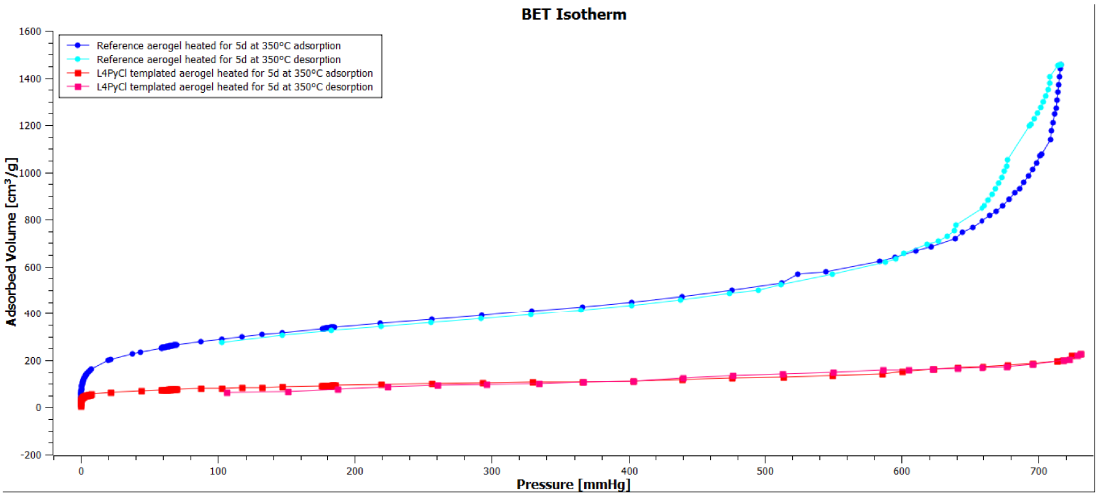

Figure 30: BET isotherms of heated aerogel and template modified heated aerogel.

IR-Measurements:

IR-Measurements result in data about local motions of the present functional groups and their concentrations in samples. The measured signals come from infra red absorption of molecules. The adsorbed energy induces molecular vibrations and most clearly in gas phases molecular rotations. Due to mass distribution and atom binding forces, the energies or wavelengths where absorption of infra red light is recognized are characteristic of functional groups or even molecules. Considering IR-measurements as a non destroying and non modifying technique for examining samples in a fast and automatic way, it is a valuable standard technique for characterising solid materials. There are several methods of recording IR-Spectra which are for the most part of only technical interest. One of these methods to differentiate are one or two beam systems. In a two beam system the beam is either splitted or redirected to another path, where a reference sample is measured in the system. This way the signal is always immediately compared to its reference signal. This is especially useful, if the wavelengths are separated with a grid or prisma. If the

wavelength detection is done by a Fourier transformation the spectrum is measured faster and compared with the data of a former reference measurement. Another more important differentiation of measurement methods is if a transmission signal is used where the infrared beam is passing through the sample or if a reflection mode is employed, where the infrared beam is reflected by the sample or a mixture of the sample and a filler material like potassium bromide.

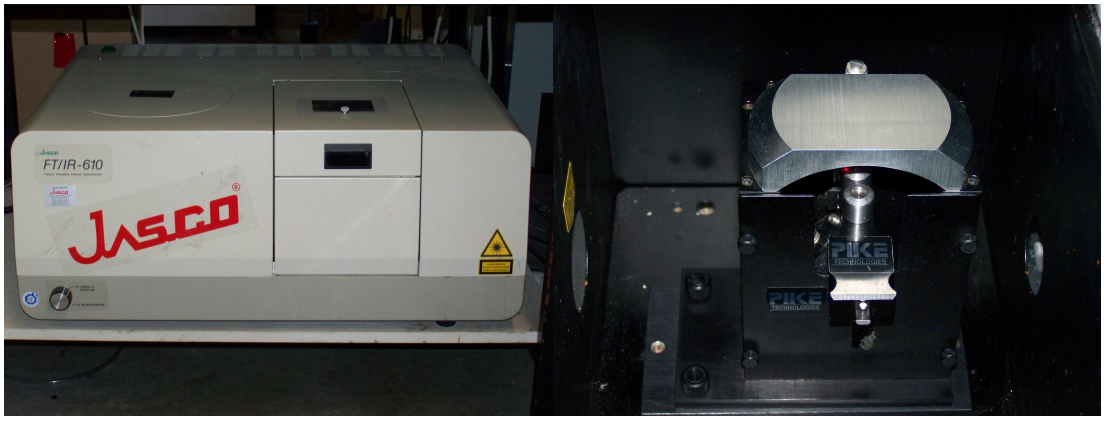

Figures 31a and b: FT/IR-610 from Jasco.

Aerogels as IR-Samples:

Aerogels are best measured in reflection mode. In order to get measurable samples, the aerogel has to be destroyed through grinding and dispersion in potassium bromide. This is mainly due to the different optical properties of different types of modified aerogel and the fact that thin aerogel samples are hard to prepare. Thicker or higher concentrated samples easily lead to total absorption of infrared light of wavelengths, resulting in no detectable signal and the loss of typical IR patterns in IR-Spectra. IR-Spectra are a valuable method for gaining information on the presence of impurities and the ratios of Si-O-Si and Si-OH groups that occur frequently in silica based aerogel.

Transmission Electron Microscopy:

Transmission electron microscopy works much like normal microscopy. In fact instead of light electrons are used to project a bigger image of the sample structure. A thin sheet of a sample is penetrated by an electron beam where heavier elements and more dense areas absorb or scatter electrons resulting in a projected picture of the sample. In order to get enough electrons through the sample, it has to be sufficiently thin, which means a thickness of about 50 nm. Most materials however cannot be made or handled easily in a thickness of only 50 nm. So there are several methods to prepare materials as TEM samples. A common general method for preparing TEM samples is to embed the sample in an embedding media such as epon. That can be hardened at 60°C in an oven. The resulting epon blocks can be cut to a reasonable size and finally cut into the required sample sheets through a diamond knife in an ultramicrotome.

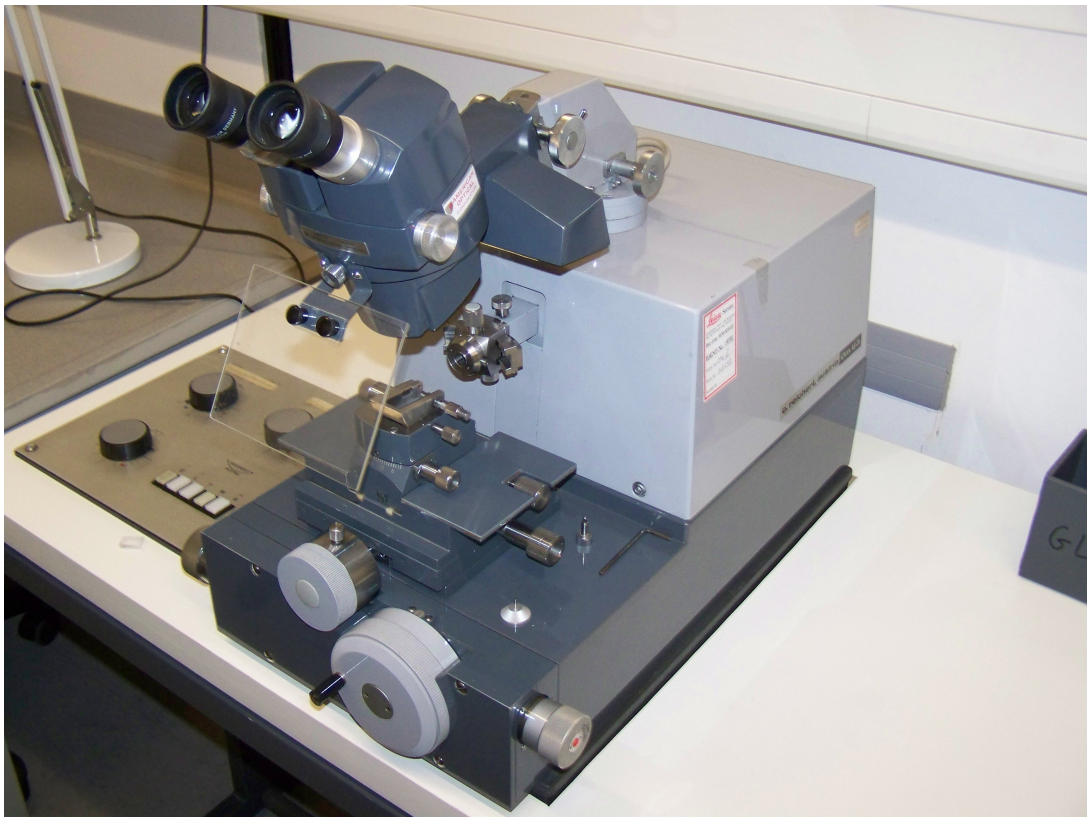

Figure 32: Ultramicrotome for cutting epon slices.

The resulting sheets are floating in a water bath and can be brought onto copper grids of 3mm diameter that are commonly used as sample holders in transmission electron microscopy. These samples can then be measured. However, it has to be noted that embedding a material in epon that solidifies in the oven and changes itself may also change the sample to some extent. So the results are always to be checked and considered as one view of the measured sample. Another method for preparing samples is to grind the material to a powder that is thin enough for transmission electron microscopy. This powder can be dispersed in a solvent and filtered through a carbon coated copper grid that works as a sample holder. It is obvious that one cannot measure dense material or bigger amounts with such a sample.

Figure 33: Transmission electron microscope (TEM) FEI CM12.

Aerogels as Transmission Electron Microscopy Samples:

In case of aerogel which consists of a sponge-like system both ways of preparing

samples work. It must be kept in mind that even the method of grinding the sample and dispersing it in solvent bears the possibility of measuring a further altered sample that only gives one view of how the system looks like. Especially grinding a sample can destroy information on a certain level of size and shape of the aerogel. Dispersion in solvent introduces a considerable amount of stress to the aerogel through capillaric forces that can further damage the aerogel and may lead to altered views in the TEM. Therefore it is a good way to employ both methods of sample preparation in order to get a better impression of how the measured system really looks like. None the less transmission electron microscopy is a valuable method for providing high resolution images in high magnifications and adds detailed information of ground samples as well as a better view of the bigger distances in modified aerogels of in epon embedded samples.

Scanning Electron Microscopy:

Scanning electron microscopy is a way of producing pictures from the surface of samples. This is done by shooting a focused beam of electrons onto the sample and measure the effects on the sample. By moving the beam on the surface of the sample a relative position of the beam and the measured effect is known and so a map or picture of the effect is made. However there are many effects that can occur when a sample is hit by an electron beam. The most obvious ones are that the electrons are reflected, absorbed or throw out other electrons from the sample. Reflected electrons are measured through a backscattered electron detector (BSE), this detector can measure either a so called material contrast (mainly if the sample is totally flat) where the strength of the signal shows which kind of material or elements are hit or, if the direction of the detected electrons is taken into account, the surface shape is

emphasized on the micrograph. Another kind of signal is the current of the sample to a ground potential showing also some material contrast on flat conductive samples.

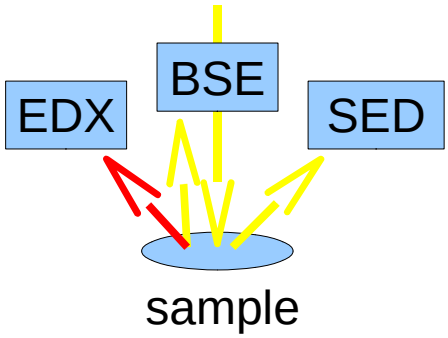

Figure 34: Showing electron beam and signals.

However the most important signal for taking and interpreting pictures is the secondary electron detector (SED) which attracts and detects electrons mostly originating from the sample. This method has the advantage of an edge-effect, that means that electrons that leave the sample and are accelerated towards the secondary electron detector have a higher chance of escaping the sample and hit the detector when the electron is originated from an edge of the sample. This results in a higher signal of electrons for edges, which especially emphasizes the shape of the measured sample. It is sensitive to charges on the sample surface. Therefore it is sometimes necessary to cover insulating samples with conducting material as carbon or a metal coating such as gold. Heavier materials also increase the contrast of this method. Another effect that can be measured is emitted x-ray radiation that comes from the replacement of thrown out electrons through electrons of higher shells in the atom. The energy of such an X-ray signal is characteristic for a certain element. This effect is measured with the energy dispersive X-ray spectroscopy (EDX). With this method a qualitative and even quantitative method is at hand for determining the chemical

elements of the sample. The quantitative results from this method are dependent on many measurement parameters as material, take off angle from the sample and energy of the electron beam. Especially the take off angle can vary significantly for non flat samples. However, this method is also used for non flat samples, but it is to be noted that this decreases the accuracy of the results.

Figures 35a and b: Scanning electron microscope (SEM) FEI Quanta 400 F with EDAX Genesis 2000 EDX System attached and (SEM) Zeis Gemini 1530.

Aerogels as Scanning Electron Microscopy Samples:

Considering the sponge-like structure of amorphous silica aerogel and the thermal and electric insulating properties as well as the very low density of silica aerogel this method of characterizing seems quite bad for getting information on the sponginess of the aerogel. However as an additional method for detecting impurities and the composition of the sample, SEM is a good method. The method provides valuable

information on sample shape that is otherwise hardly measured, especially when the aerogel is greatly altered in terms of shape such as introduced chirality. EDX was used to check the removal of structuring templates and the purity of the samples after drying or heat treatment.

Sample preparation for SEM typically consists of bringing material onto a conductive and adhesive tape on a metal plate. If the shape is important and charging effects are to be minimized the sample can be sputtered with a metal such as gold in an argon atmosphere. This provides a conductive sample surface that also increases picture contrast, but can be seen in high resolution images. It is obviously not possible to detect element compositions of sputtered samples as the metal on the surface disturbs the measurements.

Results of Template Based Aerogels Compared to Reference Aerogels

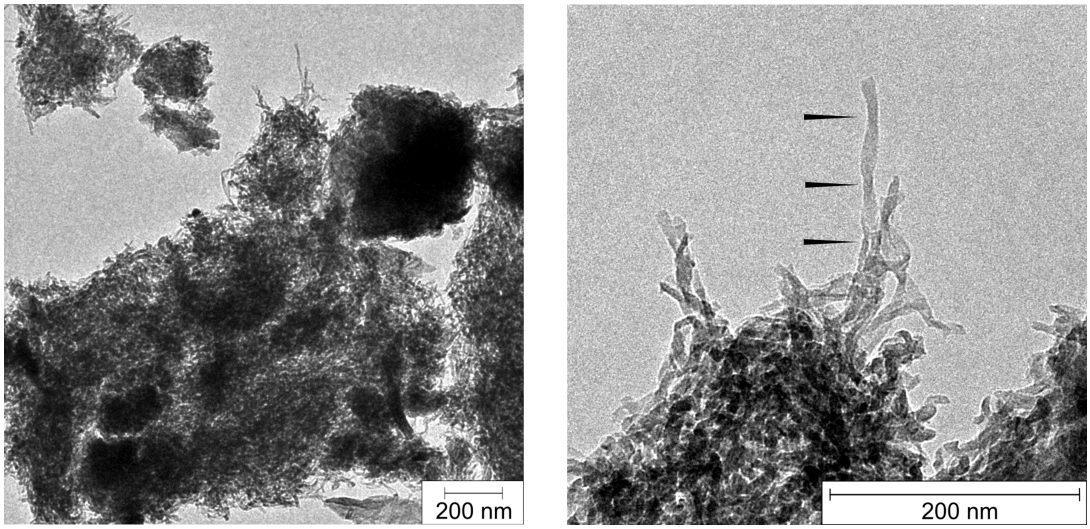

Figure 36: TEM-micrographs of the surfactant templated aerogel as ground samples on carbon coated copper-grids. In the image on the right the twistings are marked.

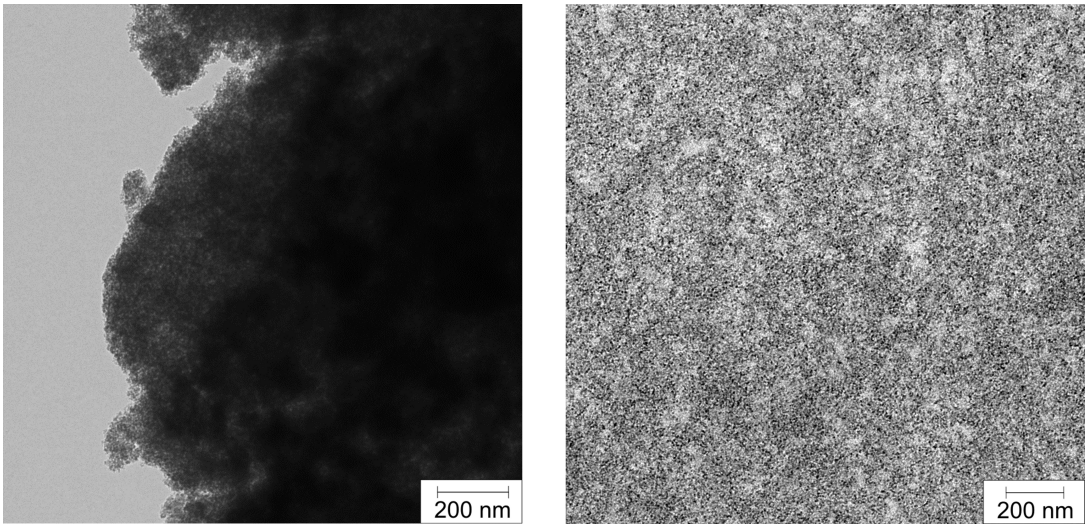

Figure 37: TEM-micrographs of surfactant-free reference aerogels. The left microgrph shows a ground sample on a carbon coated copper-grid. The right micrograph consists of a ultrathin section of a sample embedded in the epoxy resin epon (thickness about 50nm).

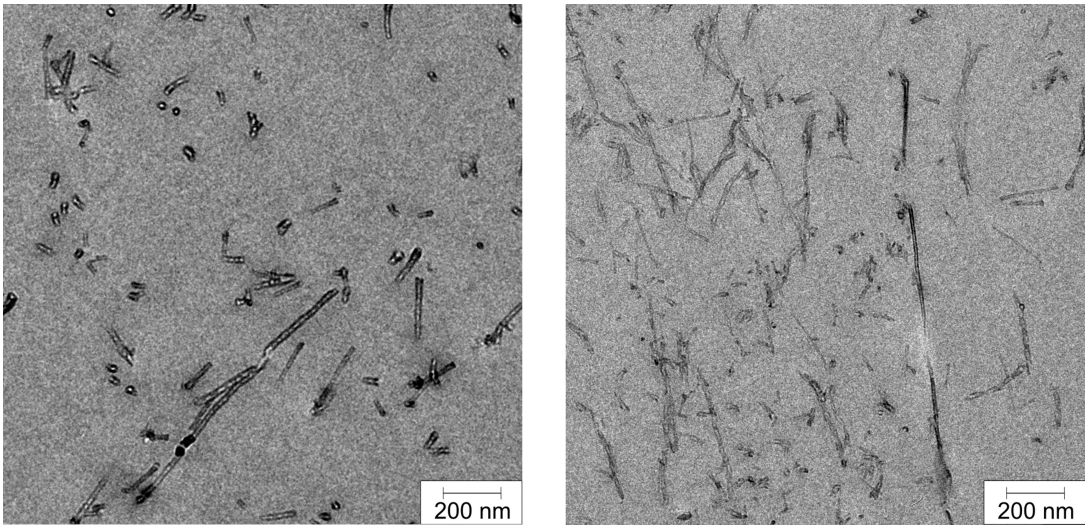

Figure 38: TEM-micrographs of the modified aerogel embedded in epoxy resin epon as ultrathin sections of about 50nm thickness.

The ground samples on carbon coated grids shown in TEM micrographs (Figure 36) consist of a network of ribbon-like fibres in contrast to the sponge like reference aerogel (Figure 37). This clearly shows the influence of the surfactant. The ultrathin

sections (Figure 38) additionally show a loose low-density network. From the SEM pictures it can be deduced that there are also additional sheet-like structures in the aerogels. Micrographs taken after heat treatment of the samples up to 350°C show that this treatment does not change the morphology of the samples. Most interestingly, a closer look at the twisted fibres (about 30 nm in diameter and up to several hundred nanometers in length) reveals that they are chiral and lefthanded with a pitch of about 100 nm (Figures 39 and 40). We managed to identify over 40 of the helical fibres as left handed, while no right handed ones were found.

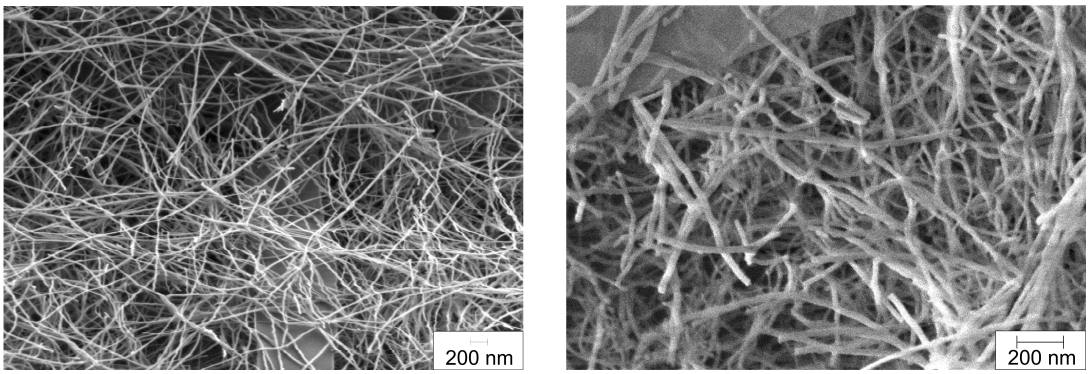

Figure 39: HR-SEM images of the template based aerogel (left image by Zeiss Ultra Plus, right image by Zeiss Gemini 1530).

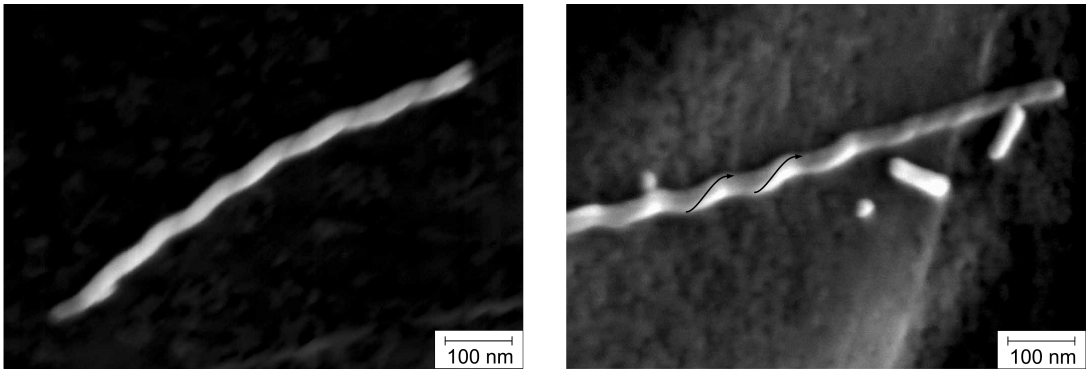

Figure 40: HR-SEM images by Zeis Ultra Plus of the surfactant templated aerogel showing left handed fibres.

To characterize the composition of the gels, EDX experiments were performed. The results, as given in table 2, reveal that the amount of carbon after heating is lower and almost as low as in the reference gel. Interestingly, there is also some carbon left in the reference sample. This might result from impurities due to adsorptive properties of silica aerogel. However, it should be kept in mind that EDX measurements do not yield precise and absolute quantitative values.

Table 2: Element composition of the aerogel samples with and without surfactant loading before and after heat treatment.

		C [at%]	O [at%]	Si [at%]
Reference AG	**Supercritical drying**	7	59	33
	Freeze drying	13	47	39
L-4PyCl modified AG	**Supercritical drying**	39	35	26
	Supercritical drying and heating	8	52	41
	Freeze drying	13	44	43
	Freeze drying and heating	6	49	45

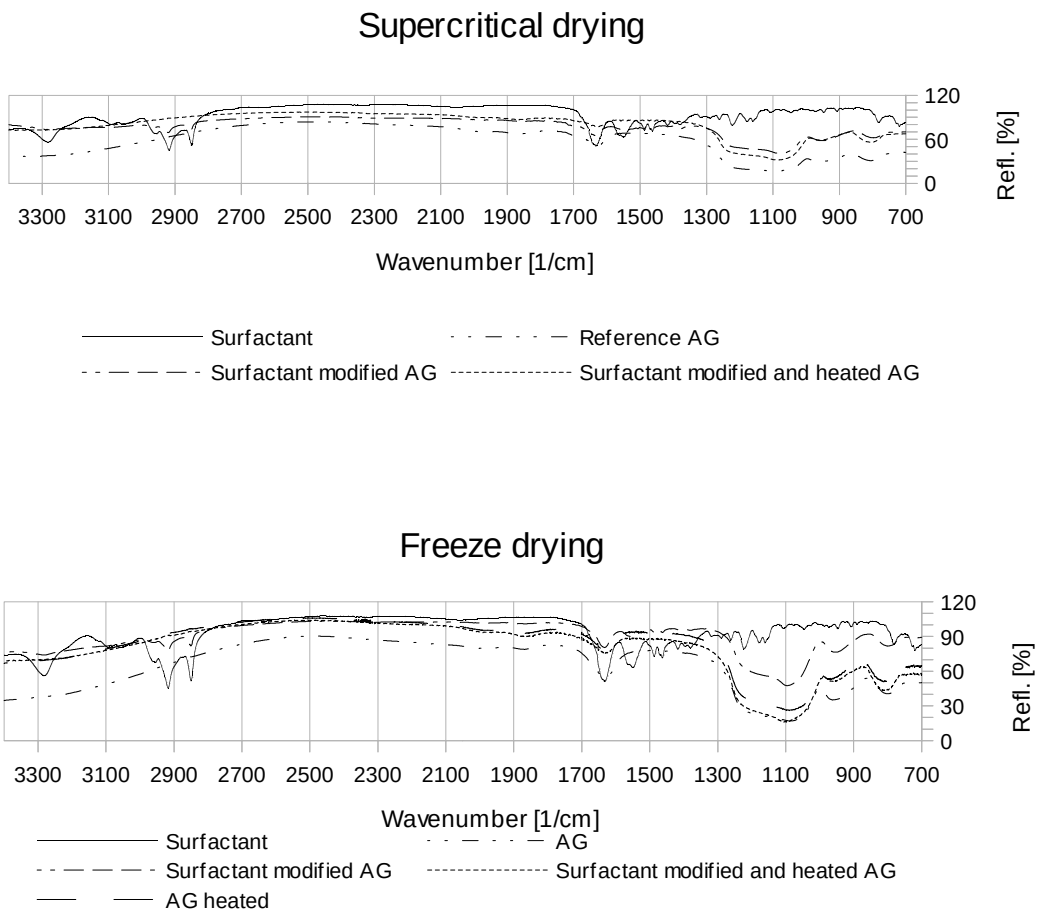

Figure 41: IR-spectra showing residual template surfactant L-4PyCl in the aerogels (AG).

Table 3: IR-spectra peaks and interpretation.

Wavenumber [1/cm]	Interpretation
3375	OH
1635	Water
1090	SiO_2 stretch
957	Si-OH
805	SiO_2 bend
1300 - 1600	Organic peaks
2800 - 3500	Organic peaks

The composition of the gels was further investigated by IR measurements as shown in figure 41. All spectra exhibit the typical silica peaks[17] (Table 3). For reference, the pure L-4PyCl compound was also investigated. Comparison of the spectra shows peaks of L-4PyCl only in surfactant modified and not heated samples, which is in

agreement with EDX-data and is another evidence that heat treatment removes the surfactant template. As expected, the solvent removal with supercritical CO_2 or freeze drying shows no difference regarding the IR results after heating the samples.

Table 4: BET results.

		Surface area [m2/g]		Total pore volume [cm^3/g]	Average pore diameter [nm]
		BET	Langmuir		
Reference AG	**Supercritical drying**	669	803	2.2253	13.3
	Freeze drying	716	959	0.5290	3.0
L-4PyCl modified AG	**Supercritical drying**	4	5	0.0035	3.7
	Supercritical drying and heating	183	246	0.1999	4.4
	Freeze drying	177	233	0.1110	2.5
	Freeze drying and heating	169	227	0.1280	3.0

In table 4 the BET surface areas and the Langmuir surface areas are given, as well as the total pore volumes and the average pore diameters. The BET measurements were performed on the unmodified reference gel (without surfactant) and the surfactant-templated gels, non-heated and heated for 5 days to 350°C. As expected, with the different structure the surfactant modification leads to a very pronounced decrease in surface area and pore volume, both being partially recovered after heating. Remind that, in contrast to xerogels, the aerogels do not significantly shrink during supercritical drying and heat treatment.

The total pore volumes and average pore diameters apparently are much higher in the untreated reference gel. However, this result is somewhat misleading, because with the applied method pore sizes above about 76 nm cannot be measured so that the vast space between the fibres is not measured as pore volume. As a consequence the small detected pores are very probably within the tiny fibres (width about 30 nm), and not between them. A more precise determination of the three-dimensional architecture

and the resulting volumes might be possible using either electron tomography (from tilt series of semi-thin sections), or via focused ion beam (FIB)-SEM analyses.

The EDX and IR data suggest that heating does not significantly influence the silica structure. However, the surfactant templated aerogels are opaque even after heating, in contrast to the transparent reference aerogel. This is probably due to the fact that the samples still contain a certain amount of organic material, especially inside the fibres. The change in morphology could also contribute to an opaque color.

Table 5: Aerogel densities.

		Density [g/cm^3]
Reference AG	**Supercritical drying**	0.107
	Freeze drying	0.043
L-4PyCl modified AG	**Supercritical drying**	0.034
	Supercritical drying and heating	0.009
	Freeze drying	0.024
	Freeze drying and heating	0.025

The densities of the aerogels are shown in table 5. As expected, the densities of the heated samples are lower than those of the non heated samples. Note that despite of similar amounts of silica precursors, much lower densities are obtained with the surfactant templated aerogels. Hence some of the silica material must have been removed during the solvent exchange and drying process. Despite their lower density they are easier to handle and mechanically more stable. This can be observed by using the more violent freeze drying method on the gels. The modified gels do not break as easily and, if they break, they break into larger fragments than in the case of the unmodified freeze dried reference aerogels.

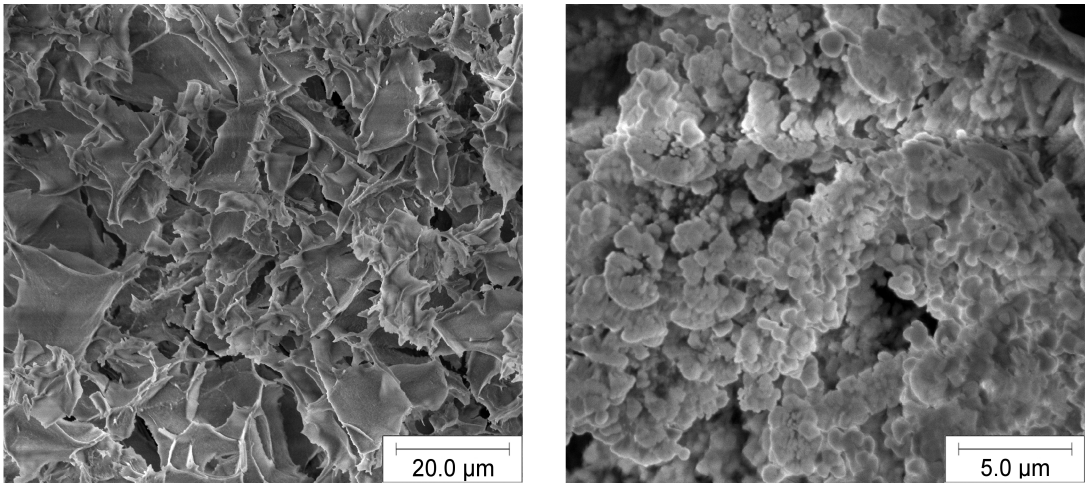

Figures 42a and b: SEM-pictures of a freeze dried reference aerogel sample on the left and a surfactant-templated freeze dried aerogel on the right side.

Freeze drying the gel after freezing in liquid nitrogen results in fissures in the reference gel most likely due to the slow freezing rate of this coolant (Figure 42a). The modified aerogel is also crumbled to smaller structures (Figure 42b). This explains why reference aerogels are opaque white after freeze drying. Otherwise the structure seems similar to the results of aerogels prepared with supercritical CO_2. Note that fissures and crumbling naturally occur at various scales resulting in much reduced lengths of the helical silica fibres in the surfactant templated aerogel.

Conclusions

Figure 43: Digital image of (from left to right) surfactant-templated supercritically dried aerogel, surfactant-templated freeze dried aerogel, freeze dried reference aerogel and supercritically dried reference aerogel (transparent).

Chiral helical fibres of about 30 nm in diameter and several hundreds of nm in length are formed as gels, using an amino acid based pyrinidinium chloride cationic surfactant. These structures sustain supercritical drying without significant changes in shape or size resulting in a new chiral aerogel. It has been shown that heat treatment of 350°C for several days removes the organic template without disturbing the aerogel morphology. The surfactant templated aerogel is different in shape and properties from reference silica aerogels. The chiral heated gels show lower surface areas and pore sizes as well as lower density. Surprisingly, the surfactant based chiral aerogels are mechanically more stable than the unmodified reference ones, despite their lower density. (Figure 43)

Sorption:

As substances with a high surface area aerogels are well suited for applications of adsorption or desorption phenomena. The high costs of aerogel synthesis with its supercritical drying process that needs high pressure and an autoclave restrict its use to fields where function and properties are more important than costs. As there has been research in applying aerogels as drug delivery systems in medicine,[7,8,23,24] it is evident that there is at least general interest in sorption phenomena. A first approach in this field was in loading a normal amorphous silica aerogel with a perfume like substance in the autoclave with supercritical carbon dioxide. The substance of choice for the experiment was geraniol as it could be easily detected and is suitable as a model substance for a perfume. The geraniol was put in the autoclave together with a normal supercritically dried aerogel. The autoclave was brought to conditions ensuring the presence of supercritical carbon dioxide namely to about 100 bars of pressure and 40°C of temperature. The system was given time to distribute the dissolved geraniol inside the autoclave and the aerogel. After this the outlet valve was opened to slowly release the carbon dioxide without inducing cracks or ruptures into the aerogel. At ambient pressure but still at 40°C the autoclave was opened to remove the now geraniol loaded aerogel. The aerogel turned yellow in the process and smells strongly of gerianol. It is soaked with geraniol and appears to be greasy and fragile. Despite of the unpleasant appearance and properties of the geraniol loaded aerogel, I decided to make desorption experiments with a thermogravimetric analyser (TGA 7 from Perkin Elmer). Under a flow of nitrogen with 25 ml/min and about 35°C the mass was measured over time to determine the desorption rate

(Figure 44). Due to the loading of the aerogel in the autoclave it was not possible to determine how much geraniol was loaded onto the silica based aerogel. In consequence it was therefore not possible to measure the amount of geraniol that stayed in the loaded aerogel. In consequence the TGA – results yield no absolute values but show trends. In order to customize the release rate of geraniol the surface of silica aerogel was hydrophobised by heating under nitrogen atmosphere. The results clearly show a trend of higher release rates of more hydrophobic silica aerogels. The obtained data for liquid geraniol without any aerogel fit the model of hydrophilic aerogel decreases release rates as hydrophobic aerogel increses release rates of adsorbed geraniol.

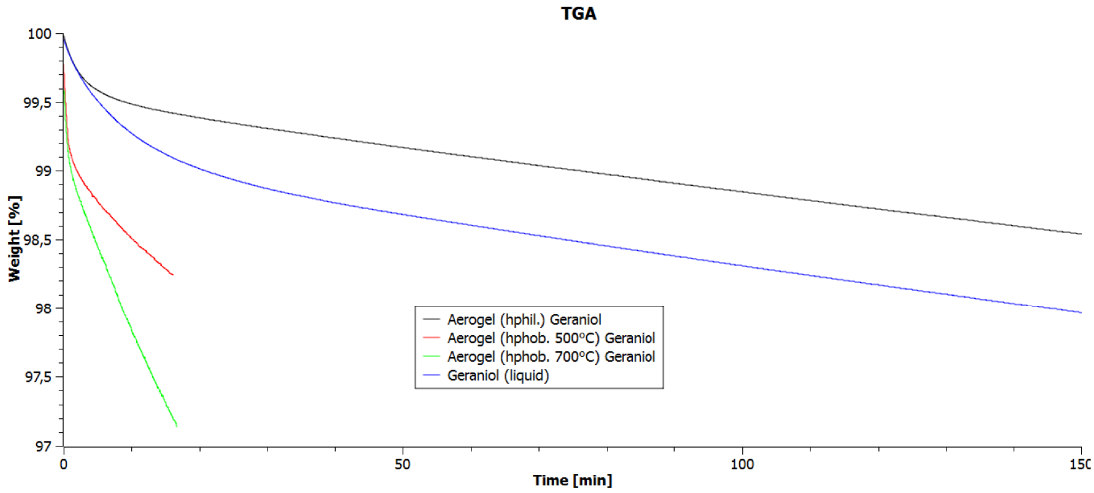

Figure 44: Desorption of geraniol from geraniol loaded aerogels and liquid geraniol.

Some further experiments have been made to examine the release properties in presence of water that is known to crack and dissolve the gel. It could be shown that in the presence of water the release rate of geraniol from silica based amorphous aerogel is increased as shown in figure 45.

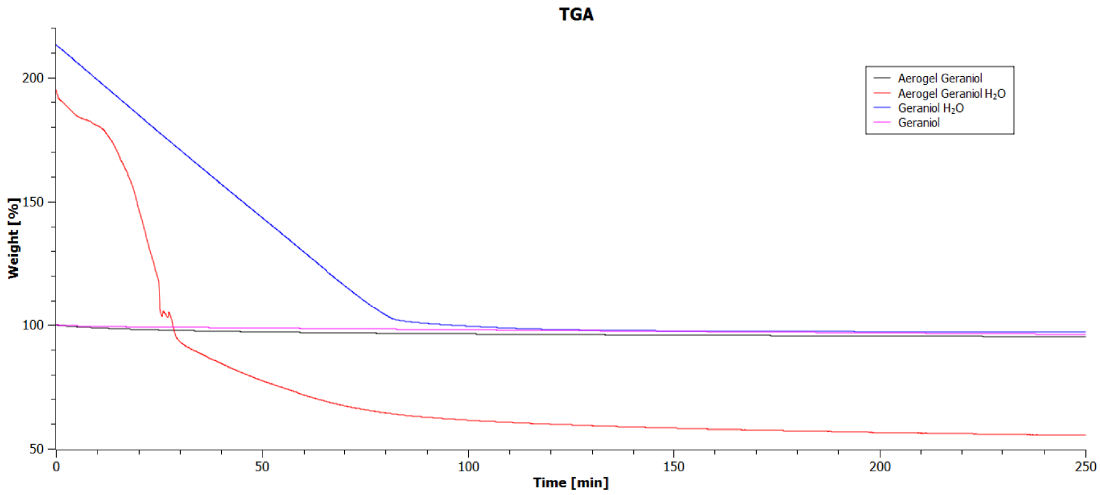

Figure 45: Showing the increased desorption rate of geraniol from aerogels with added water.

Due to the unpleasant material that decrease the possibilities of application and the problems during the measurements I decided to use a more general approach in applying adsorption measurements in order to predict sorption properties of aerogels. In order to predict the adsorption of material on aerogels an empirical method was chosen to fit measured adsorption data to molecular property data from COSMO and COSMO-RS calculations.

COSMO: The Conductor like Screening Model

When experiments are time and cost intensive it is often tried to simulate or calculate the properties of interest. So it is not surprising that quantum chemical methods are applied when it comes to property predictions. Especially in the beginning of applying this methods computational abilities were limited to single molecules with only a handful of atoms. Thus calculations were and are still somewhat limited to modelling more or less isolated molecules in gas phase. However as the research in microelectronics and chip design produced more capable hardware the number of

atoms that can be reasonably calculated with quantum physics rose and so the look into how other more interesting phases than the gas phase could be investigated began. The attempt resulted in the use of reoccurring patterns in crystals that can be calculated if symmetry is used to keep the number of atoms in the calculated system small. With the ability of calculating gas phase and certain crystal phases, calculations of less ordered solids and the especially interesting liquid phase is still hard and mostly done by employing molecular dynamics or group contribution methods in order to get properties of the calculated system. The conductor like screening model (COSMO) takes a similar approach as first quantum physical models when it comes to calculate isolated molecules. In the liquid phase most systems are not ordered like a crystal, so boundary conditions have to be calculated in a different way. Klamt et. al took a different approach in calculating the molecule in a cavity of an ideal conductor. The properties of interest from the calculation are not only the positions of the atoms. The most interesting part for further calculations are the electrostatic values on a shell with certain empirical found distances from the atoms that can be interpreted as the molecules border interface to solvents or other molecules. Examples of such surfaces are depicted in figures 46a-d.

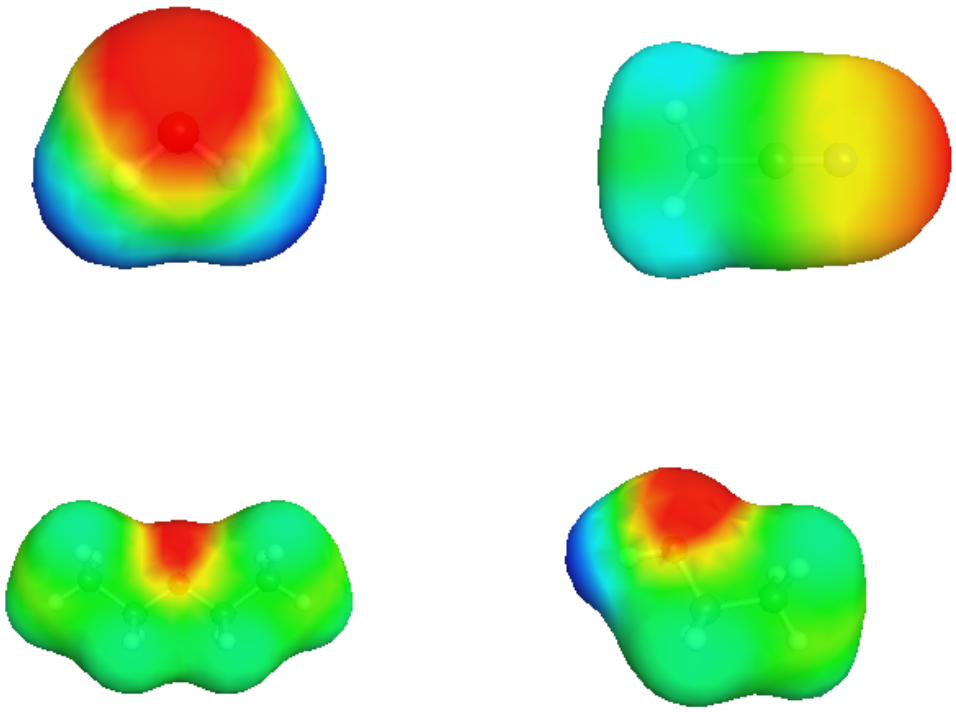

Figures 46a-d: Sigma-surfaces of water (upper left), acetonitrile (upper right), diethylether (lower left) and ethanol (lower right).

Treating the surrounding environment of the calculated molecule as a continuum the intermolecular interactions are not fully taken into consideration leaving some space for improvement. This leads to a necessary extension to this approach where molecular interactions are considered more deeply. COSMO-RS is such an extension. But before explaining COSMO-RS the benefits and drawbacks of this approach should be pointed out. By still considering only isolated molecules in quantum chemistry the number of atoms that must be calculated is still small and manageable with reasonable time and resources, as mixtures are later calculated from the properties of single molecules. Not only the number of atoms calculated is small compared to molecular dynamic models within this approach. It is also not necessary

to recalculate a molecule for different concentrations or mixtures. Once calculated results can be stored in a database for later use. This approach also makes it possible to calculate systems with molecules that contain many atoms with reasonable effort.

COSMO-RS: A Calculation Method for Intermolecular Interactions.

COSMO-RS is a model for calculating intermolecular interactions. With this interaction model it is possible to calculate properties of mixtures of molecules such as solutions or gas mixtures. The base of the calculations is the electrostatic information on the molecule shell from the COSMO calculations. For the energy of the system the fitness of the surface-surface fragments is calculated. To combine this information with the molecules present in the system the surface fragments are weighted by the molar ratios and summed up to a sigma profile as shown in figure 47. It is to note here that a negative σ value represents a positive polarity and a positive σ stands for a negative polarity. A low σ value indicates areas with low polarity.

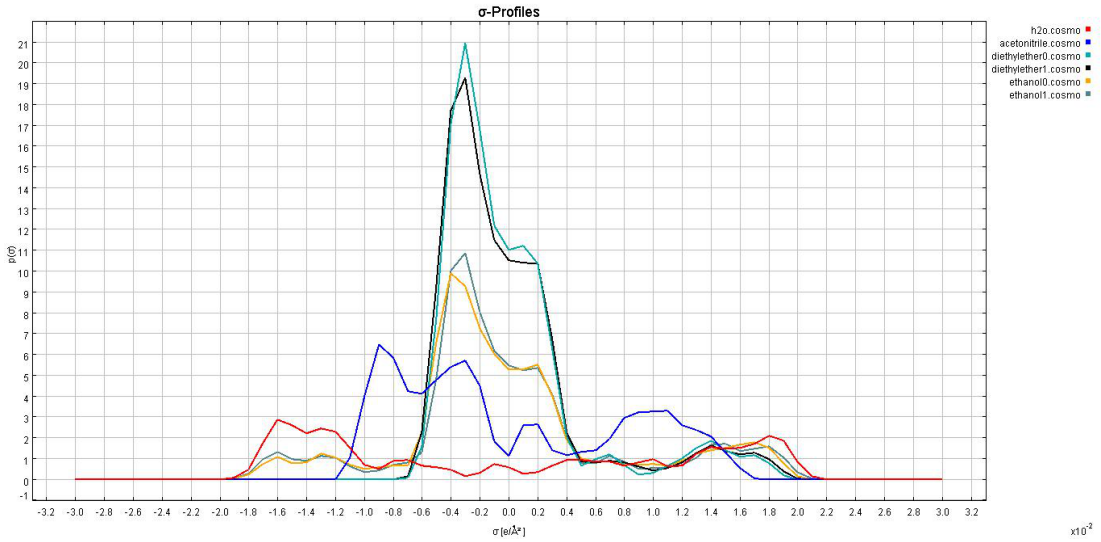

Figure 47: Showing sigma-profiles of some molecules. Certain molecules as ethanol have different possible conformations that result in different curves. The x-axis shows the electrostatic polarity σ of a certain surface fragment while the y-axis shows the number of occurances in the system.

From pairing the surface fragments it is possible to calculate the energy of the system. The calculated energies build the next result of COSMO-RS calculations called a sigma potential (Figure 48).

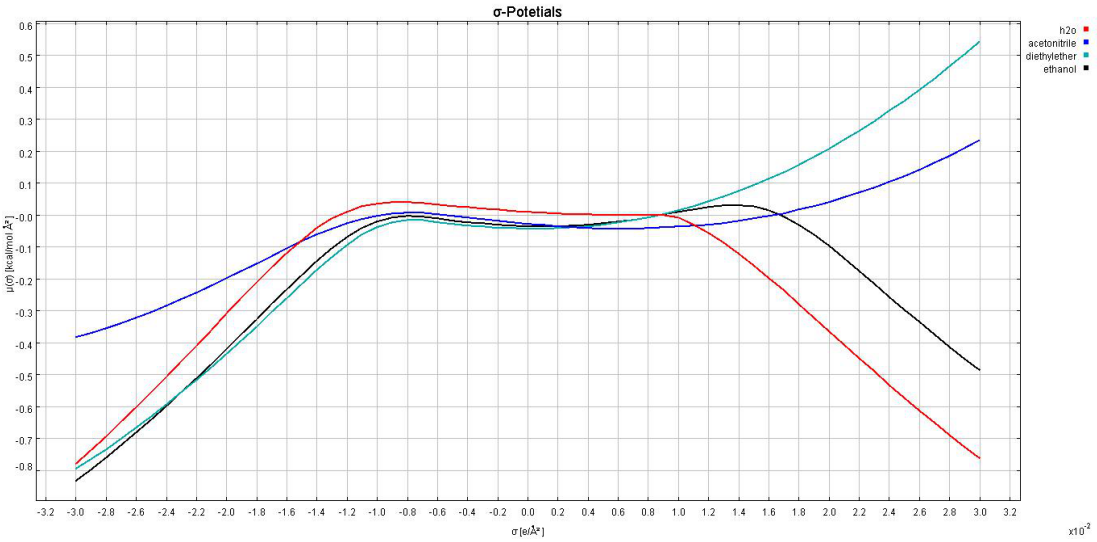

Figure 48: Showing sigma-potentials of example molecules. The x-axis shows the electrostatic polarity sigma of a certain surface fragment while the y-axis shows the chemical potential in the system.

These sigma potentials can be calculated for pure substances as well as for mixtures. As the surface fragments for an electrostatic value are summed up, distance information between the surface fragments are lost for pairing them. This is a reasonable simplification if steric considerations are negligible. The sigma profile and sigma potential distributions however can be valuable diagrams for estimating the properties of molecules. And therefore it is not surprising that, if the sigma potential is parametrized, some of the values can be correlated to molecular properties. This has been realized by introducing the so called sigma moments that are indeed values from such a parametrisation. Moment 0 is correlated to the surface of the molecule. Moment 1 represents the negative value of the charge of the molecule. There have also been introduced sigma moments that represent values for proton acceptors and donors in the molecules. With this system it has been shown that calculations of surface interactions can be done on an empirical base. Especially

in the field of adsorption it has been shown that empirical measurements can be used to fit a linear combination of the sigma moments with parameters resulting in an equation for predicting measurement outcomes for different molecules. All this is possible without knowing the composition of the adsorbing material. This is especially useful for materials that are hard to characterize as shown with soil[25] or charcoal[26]. The use of σ-moments and their physical interpretability offer additional possibilities in understanding which parameters are important for adsorption properties. For example, it provides useful information about the nature of adsorbents, like the presence of charges or donors and acceptors. In the following chapter this approach was also used to predict adsorption of substances to aerogels.

Adsorption on Silica Aerogels as Predicted by COSMO-RS σ-Moments

Adsorption and desorption properties have been an important field in chemistry for a long time. Their importance is evident from their widespread practical use in different fields, such as analysis and purification in chromatography, filtering and release of substrates in parfume industry or medicine to name only a few examples.[7,8,23,24] Not surprisingly many experiments are done in order to characterize adsorption properties. This vast amount of experiments is time consuming and expensive. Therefore attempts have been made to predict these properties from calculations. On the other hand theoretical calculations alone can be complicated or impossible to perform, because of impurities or adsorbents that are not fully characterized or representable with a mixture of simple molecules.

Nevertheless, there have been successful attempts to derive these properties from a

small subset of experiments in order to correlate the existing data with molecular descriptors from adsorbates, like the prediction of soil sorption coefficients,[25] blood-brain partitioning[27] or adsorption on activated carbon.[26] These experiments have shown that calculations based on a restricted empirical data set are a real alternative and sometimes the only possibility for prediction of adsorption properties in complex, real world applications.

The Investigated Systems

The adsorbents used were silica aerogel and surfactant templated modification of a silica aerogel, providing different properties. The synthesis and characterisation of these gels has already been shown in this work and is extended here as it is important for our adsorption experiments. In order to be able to reuse the same samples for many adsorption experiments and in order to remove any remaining residues from the gel samples these samples were heated to 350°C for 5 days after drying in order to remove the organic material as the surfactant in templated aerogels. Between the adsorption measurements the samples were also heated to 350°C until no weight change was observed.

Adsorption Measurements

For simplicity and according to the fragile nature of aerogels we measured the adsorption from a gas phase over a liquid phase of adsorbates at about 25°C. Each adsorbate was measured in a separate experiment. The experiments for the two aerogels where run in parallel with adsorbents having contact to the same gas phase until a constant weight of the aerogels were reached. The weight of the adsorbate was divided by the weight of the adsorbent to get the adsorption coefficient. In order to

get comparable results we considered vapor pressures and molecular weights of the adsorbates, and divided the adsorption coefficients by these values.

Derivation of the Working Equation for the Prediction of Adsorption Values

As shown in equation I the partition coefficient $K^X_{S,S'}$ is connected to the difference of the chemical potentials μ of the adsorbate X in the phases S and S'. The equation also contains the temperature T and the Boltzmann constant k.

$$kT \ln K^X_{S,S'} = [\mu^X_{S'} - \mu^X_S] \tag{I}$$

The chemical potential of a substance X in or adsorbed on a phase S or S' can be calculated with the COSMO-RS approach from a small combinatorial contribution that comes from size effects and an integral over the surface composition function p and the chemical potential as a function of σ (see equation II).

$$\mu^X_S = \mu^X_{S,comb.} + \int p^X(\sigma)\mu_S(\sigma)\, d\sigma \tag{II}$$

It has been been shown that σ-potentials can be described as a Taylor-like expansion, c. f. equation III.[25–28]

$$\mu_S(\sigma) \approx \sum_{i=-2}^{m} (c^i_S f_i(\sigma)) \tag{III}$$

with m as the size of the Taylor-like expansion reduced by 2.

$$f_i(\sigma) = \sigma^i \quad \text{for } i \geq 0 \tag{IVa}$$

$$f_{-2}(\sigma) = f_{acc}(\sigma) = \begin{cases} 0 & \text{if } \sigma \leq \sigma_{HB} \\ \sigma_{HB} - \sigma & \text{if } \sigma > \sigma_{HB} \end{cases} \tag{IVb}$$

$$f_{-1}(\sigma) = f_{don}(\sigma) = \begin{cases} 0 & \text{if } -\sigma \leq \sigma_{HB} \\ \sigma_{HB} + \sigma & \text{if } -\sigma > \sigma_{HB} \end{cases} \tag{IVc}$$

As can be seen in the equations IV a, b and c the parameters f are calculated from σ and the hydrogen bonding boundary parameter σ_{HB}. As shown in equation V the partition coefficient $K^X_{S,S'}$ can be expressed as a linear combination of σ-coefficients $c^i_{S,S'}$ and the surface composition function p^X.

$$\begin{aligned} \ln K^X_{S,S'} &= \frac{1}{kT}[c_{S,S'} + \int p^X(\sigma)(\mu_{S'}(\sigma) + \mu_S(\sigma))d\sigma] \\ &\approx \tilde{c}_{S,S'} + \int p^X(\sigma) \sum_{i=-2}^{m} \tilde{c}^i_{S,S'} f_i(\sigma) d\sigma \end{aligned} \tag{V}$$

With the introduction of the σ-moments M_i^X,

$$M_i^X = \int p^X(\sigma) f_i(\sigma)\, d\sigma \tag{VI}$$

we obtain the working equation VII, where the σ-coefficients $c^i_{S,S'}$ can be adapted to the measured partition coefficients and the calculated σ-moments M_i^X.

$$\ln K^X_{S,S'} = \tilde{c}_{S,S'} + \sum_{i=-2}^{m} (\tilde{c}^i_{S,S'} M_i^X)) \tag{VII}$$

With the σ-moments M_i^X from the COSMO-RS calculations and the logarithmic value of the adsorption properties K we can adjust the parameters c by referring to the data for each adsorbate.

Table 6: Table showing the used and predicted values, the cross-validation test sets, and the training set of all values in their division into the used folds. Abbreviations: vap. p. vapor pressure, calc. calculated, acc acceptor, don donor, cv cross-validation, pred. predicted, mod. modified, and M molecular weight.

adsorbate	σ-moment 0	2	3	acc	don	vap. p. (calc.) [mbar]	M [g/mol]	log(K) aerogel	cv pred. log(K) aerogel	pred. log(K) aerogel	log(K) mod. aerogel	cv pred. log(k) mod. aerogel	pred. log(k) mod. aerogel
ethanol	88.30	52.21	22.95	4.18	1.78	55.09	46.07	4.58	4.59	4.53	4.80	4.74	4.73
ethylacetate	133.49	53.02	35.73	2.24	0.00	76.27	88.11	4.32	4.36	4.31	4.75	4.51	4.54
benzene	121.37	27.38	-0.51	0.00	0.00	124.02	78.11	4.58	4.93	4.88	4.88	5.17	5.15
2-propanol	107.22	50.76	24.73	4.05	1.38	17.96	60.10	3.69	4.28	4.22	4.33	4.51	4.50
propanol	108.36	50.95	22.17	3.79	1.54	22.11	60.10	3.78	4.27	4.22	4.27	4.45	4.40
chloroform	117.53	26.59	-20.69	0.00	1.28	178.84	119.38	4.87	4.50	4.62	5.01	4.62	4.62
methylene chloride	98.49	32.52	-15.25	0.00	0.19	448.26	84.93	5.19	4.88	5.02	5.24	5.40	5.53
tetrahydrofuran	111.77	35.48	37.92	3.47	0.00	216.15	72.11	4.76	4.77	4.72	5.71	5.19	5.27
1-octanol	207.72	54.37	22.54	3.75	1.48	0.09	130.23	2.02	2.37	2.14	1.86	2.50	2.06
diethylether	130.48	31.02	29.95	2.55	0.00	583.40	74.12	4.72	4.49	4.50	4.99	4.94	4.89
hexylamine	172.12	50.94	54.13	5.49	0.03	12.14	101.19	3.45	2.74	3.02	3.88	3.57	3.65
water	43.06	74.84	12.67	5.69	3.85	31.69	18.02	5.09	3.94	4.58	4.55	4.34	4.48
carbon tetrachloride	134.21	9.93	-2.94	0.00	0.00	108.41	153.82	4.66	5.01	4.81	4.77	5.25	5.08
toluene	140.55	27.59	1.29	0.00	0.00	38.35	92.14	4.37	4.71	4.51	4.60	4.77	4.70
methanol	67.56	52.58	22.15	4.19	1.88	78.04	32.04	4.40	5.04	4.93	5.10	5.21	5.16
cyclohexane	131.49	5.68	0.31	0.00	0.00	289.43	84.16	5.28	4.91	4.98	5.44	5.03	5.20
methylformate	93.14	50.95	23.44	1.41	0.00	659.75	60.05	5.49	5.10	5.18	5.49	5.67	5.51
acrolein	97.90	46.57	24.72	1.84	0.00	354.13	56.06	4.96	5.00	5.05	5.26	5.59	5.45

For practical reasons the decadic logarithm was used during the calculations instead of the natural logarithm. This only changes the values of the fitted parameters and does not change the predicted values. The fitting of the data for the silica aerogel results in equation VIII, and the corresponding working equation for the surfactant templated silica aerogel is shown in equation IX.

$$log(K) = 7.761 - 0.021M_0^X - 0.014M_2^X + 0.017M_3^X - 0.261M_{acc}^X \quad \text{(VIII)}$$

(n=18, r^2=0.85, RMS=0.32, q^2=0.67, QMS=0.48)

where n is the size of the data, r^2 the regression coefficient and RMS the standard deviation (root-means-square) with its analogs for the cross-validation q^2 and QMS.

$$log(K) = 8.343 - 0.023M_0^X - 0.013M_2^X - 0.492M_{don}^X \quad \text{(IX)}$$

(n=18, r^2=0.93, RMS=0.23, q^2=0.86, QMS=0.33)

The σ-moment 1 is related to the charge of the adsorbates and hence has no influence on the equations, because all examined adsorbates have a value of zero representing no charge. In case of the modified silica aerogel the third σ-moment is not significant. This is in agreement with other predictions of partition coefficients with σ-moments such as adsorption on activated carbon, soil sorption or blood-brain partition coefficients.[25,27,28] Another remarkable result is the difference in the relevance of donor and acceptor moments between the unmodified and templated silica aerogel discussed later in this work. The resulting equations were used to predict adsorption parameters for all substances. We also performed a 4-fold cross-validation to get predictions for a larger number of test sets, see figures 49 and 50. The RMS of 0.32 for aerogel and 0.23 for the surfactant templated aerogel matches very well with the accuracy limit of 0.25 log-units generally valid for COSMO-RS models.

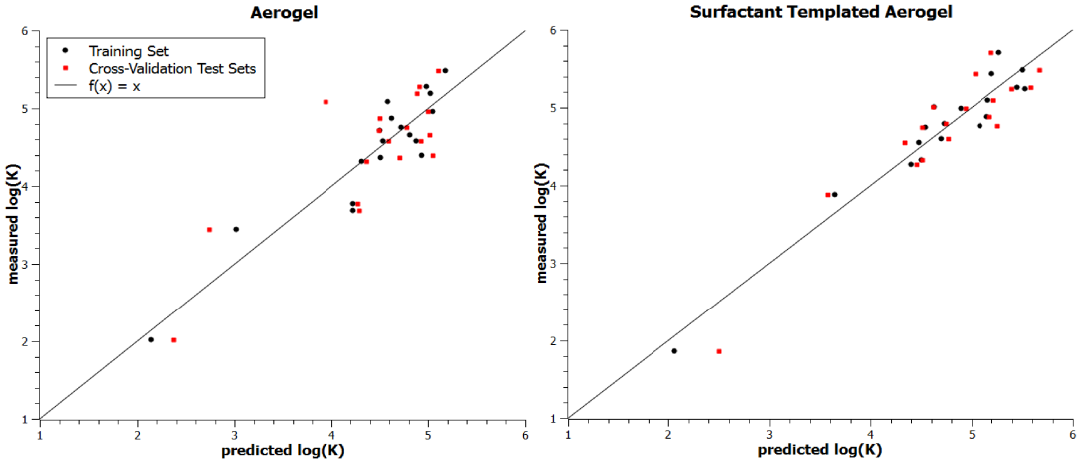

Figures 49: The figures show the predicted values compared to the actual measurements.

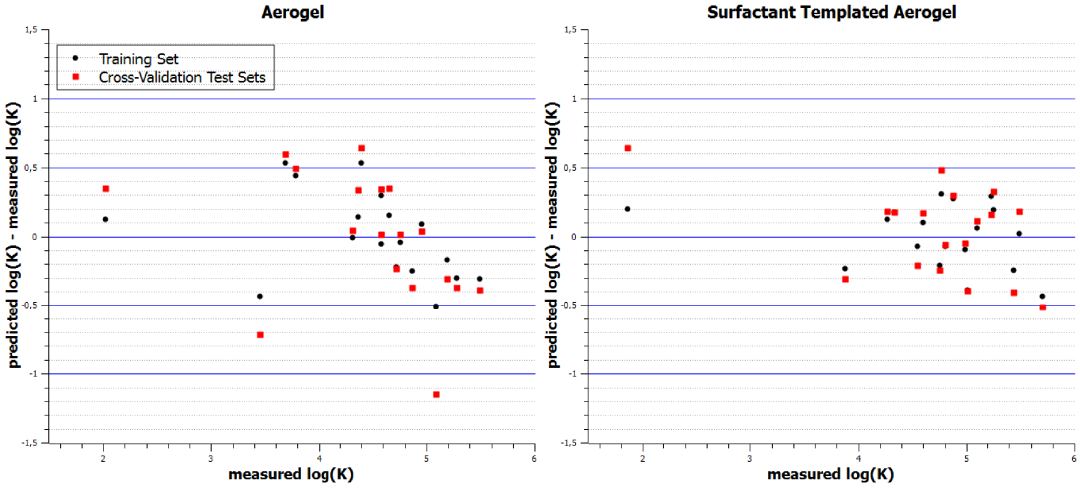

Figures 50: Showing the prediction errors compared to the actual measurements.

Interpretations

Considering the fitted equations for the two aerogels the most obvious differences are the importance of the acceptor moment M_{acc} for the unmodified aerogel in contrast to the presence of the donor moment M_{don} in the equation for the surfactant templated silica aerogel. In order to explain the importance of acceptor and donor moments, it

is important to understand the modifications of the gel. The unmodified silica aerogel has a sponge like structure. The surfactant templated aerogel is grown along the template structure of chiral helical fibres. This results in more dense helical fibres with vast distances between them (Figure 51b). As a result the surfactant templated aerogel has a smaller surface area.

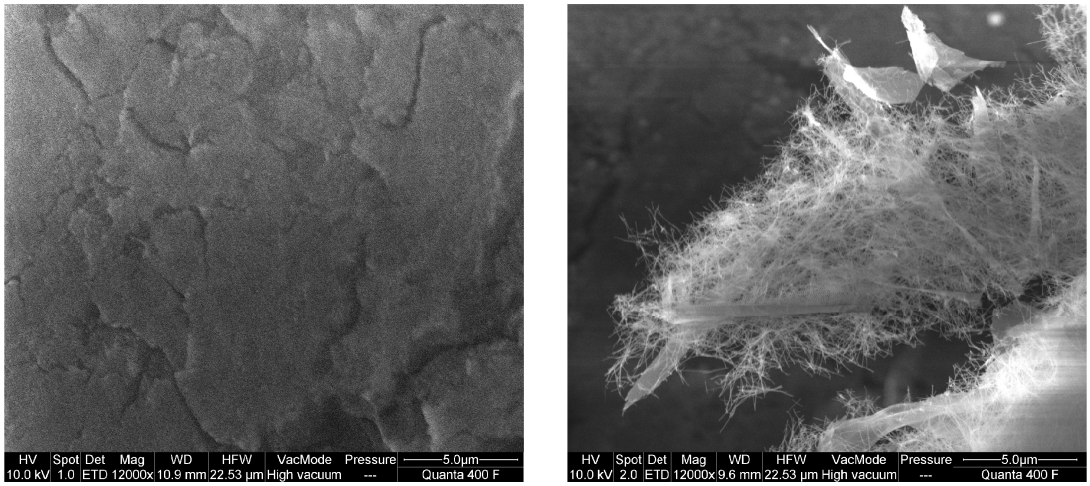

Figures 51a and b: Showing reference silica aerogel in the left and the modified silica aerogel in the right picture.

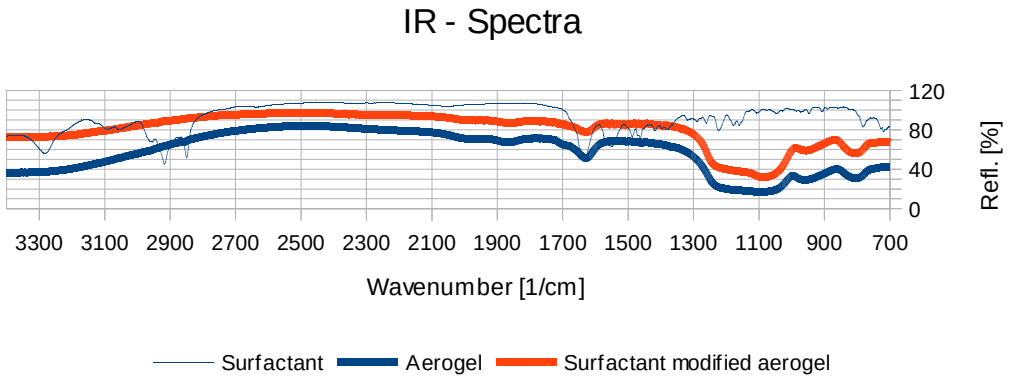

Figure 52: IR-spectra showing groups of SiOH at 957 1/cm and Si-O-Si at 1090 and 805 1/cm.

As the spectra in figure 52 show, Si-O-Si and Si-OH are the main functionalities in

amorphous silica. It should be stressed that IR reflects bulk and surface functionalities, whereas adsorption phenomena are obviously only related to surface-surface interactions. However, it can be assumed that Si-OH as terminal groups occur mostly on the surface of the aerogels. According to the IR-Spectra, there are more Si-OH groups present in the unmodified aerogel. Exposing a donor such as Si-OH groups makes the acceptor moment in adsorbates more important. As can be seen from the σ-surfaces in figure 53, the donor moment of the adsorbate is relevant for both groups, but is more pronounced with Si-OH groups. It is to note here that for COSMO calculations in COSMOthermX software only molecules are allowed. Therefore the groups were turned into molecules by adding hydrogen. However, for σ-profiles and σ-potentials (Figure 54a and b) only the group surfaces have been used.

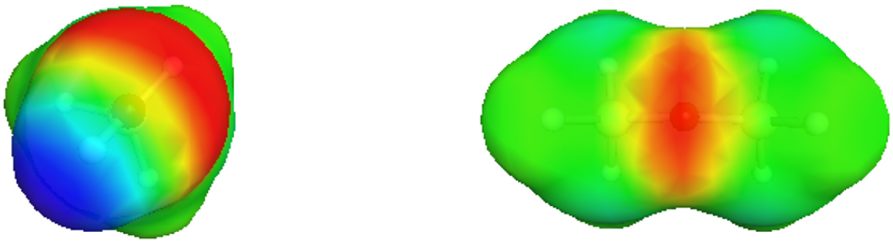

Figure 53: Top views onto the oxygen showing the σ-surface of H_3SiOH on the left and $H_3Si\text{-}O\text{-}SiH_3$ on the right.

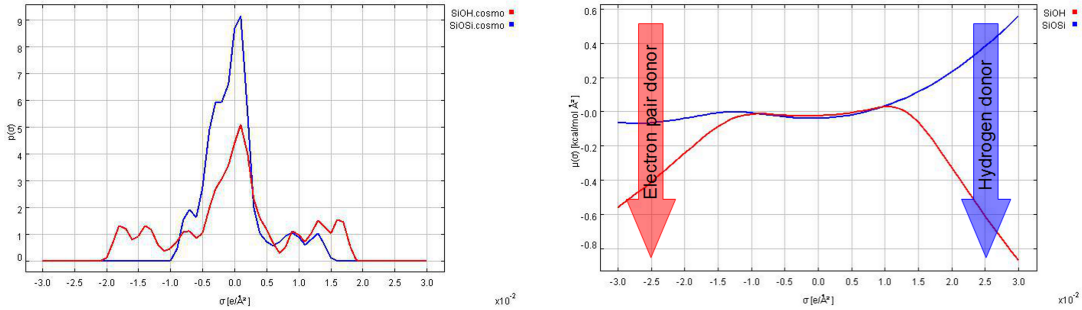

Figures 54a and b: σ-profiles on the left side and σ-potentials on the right side of possible silica surface groups.

The σ-profiles show a quantitative result of the σ-surfaces by summing over the occurrences of certain polarisation charge densities. It is to note here that a negative σ value represents a positive polarity and a positive σ stands for a negative polarity. Based on the surface-surface interactions of the polarization charge densities Klamt derives the chemical potential of surface segments, the so-called σ-potential. The σ-potential is a characteristic function for a molecule and reflects its properties. It has been shown that for uncharged molecules 5 parameters called σ-moments can be fitted to represent a fingerprint for a molecule often resembling molecular properties such as surface area, charge and polarizability. Moment M_0 is correlated with surface area and moment M_2 is correlated with polarizability. Having a closer look on the prediction equations VIII and IX, the moments M_0 and M_2 are similar in both equations. The higher moments are harder to interpret, especially when considering the big difference in acceptor and donor properties. However, it is to be noted that not all descriptors are needed for a good prediction of the surfactant templated aerogel.

Conclusions

This work is a proof of concept showing the successful prediction of adsorption properties from gas phase at saturation concentration of adsorbates for different adsorbents. The predictions and the interpretations are based on empirical data that do not require exact knowledge of the adsorbents and can therefore be used for natural as well as industrial and even impure or unknown adsorbents. It has also been shown that the resulting equations can contribute to the exploration of the adsorption phenomena and to the understanding of surface-surface interactions for the adsorbates under consideration.

Conclusions and Outlook

An autoclave has been built as part of this work. An autoclave that is capable of a relatively homogeneous influx and outflux of carbon dioxide and maintain pressure and temperature conditions needed for supercritical carbon dioxide. The autoclave has successfully been used in this work to remove solvents as acetonitrile and acetone from gels avoiding the phase barrier by using a temperature pressure path above the critical point of carbon dioxide. A second use of the autoclave in this work was the ability to “load” gels with substances soluble in supercritical carbon dioxide. Although not part of this work, it has also been used for extractions with supercritical carbon dioxide. This might be continued in combination with reactions to not only extract but extract and modify a substance simultaneously. As part of these reactions aerogels could act as supporting material for catalysts due to their porous nature. This way it could even be possible to apply catalysts that normally would not be possible due to their insolubility in supercritical carbon dioxide.

Silica gels and their synthesis have been investigated. The gels have been modified and the properties changed significantly in the resulting silica aerogels. A cationic chiral surfactant L-4PyCl (Figure 22) has been used to form self assembled templates for silica growth resulting in chiral amorphous silica gel fibres that show helical structures and sheets. This templated aerogel has been analysed together with an unmodified reference silica aerogel. Analysis methods were electron microscopy micrographs, EDX, BET and TGA, among others. These results show different properties of the templated aerogel especially in shape (in nanometer scale), lower

surface area and pores of the material. These properties seem also to influence mechanical stability as the local density of the templated aerogels seem to be higher than for a normal unmodified aerogel.

It has been shown with EDX and FT-IR measurements that heating the templated aerogel in an air atmosphere leads to removal of organic residues that could stem from the organic template, without shape change.

Additional to BET measurements sorption measurements have been made. Some of these sorption results have been used to develop a model for prediction of adsorption parameters. This model uses the COSMO-RS system and especially the σ-moments. The models show that the aerogels can be described by the resulting equations. It was further possible to interpret the resulting equations in accordance to FT-IR data of the gels concerning the presence of surface groups of the gels. This could also be seen as a kind of characterisation of the aerogels as they adsorb substances differently.

These model equations should be considered as proof of principle due to their limited data base but could be used perhaps with additional data to predict and finetune appclications of aerogels where sorption is a crucial or at least important part of its properties.

There has also been taken effort to make a tomography of the cationic surfactant templated aerogel to get a three dimensional image of its structure. This work will be

further persued and will possibly result in additional proof of the chiral helical structure of this surfactant templated aerogel.

Acknowledgements

I wish to thank Professor Klamt for many valuable discussions and Professor Schmalz, University of Regensburg for providing access to a FEI Quanta 400F scanning electron microscope with an EDAX Genesis EDX system and Martina Heider for HR-SEM measurements with a Zeiss Gemini 1530 at the University of Bayreuth, and Mr. Liron Issman for the HR-SEM work, which was performed at the Technion Laboratory for Electron Microscopy of Soft Materials, supported by the Technion Russell Berrie Nanotechnology Institute (RBNI). My thanks include the help of Professor Rachel, University of Regensburg and his team for access and support in sample preparation for TEM measurements and helpful suggestions. I thank Dr. Müller, University of Regensburg for his support and access to many devices like the BET, thermogravimetric analyzer and the fourier transform infra red spectrometer. My thanks go to Prof. Smirnova for providing the blueprints and data that made it possible to construct the autoclave and for the start in how to produce silica aerogels. I thank everyone in the workshops of the University of Regensburg that helped in this work and especially for building the autoclave. Last but not least I have to thank Professor Kunz and my colleagues for their support in this work.

References

1. Brinker, C. J. & Scherer, G. W. *Sol-Gel Science: The Physics and Chemistry of Sol-Gel Processing: The Physics and Chemistry of Sol-gel Processing*. (Academic Press, 1990). at <http://www.amazon.de/Sol-Gel-Science-Physics-Chemistry-Processing/dp/0121349705>

2. Kistler, S. S. Coherent Expanded-Aerogels. *The Journal of Physical Chemistry* **36,** 52–64 (1931).

3. Hamann, T. W., Martinson, A. B. F., Elam, J. W., Pellin, M. J. & Hupp, J. T. Aerogel Templated ZnO Dye-Sensitized Solar Cells. *Advanced Materials* **20,** 1560–1564 (2008).

4. Cantin, M. *et al.* Silica aerogels used as Cherenkov radiators. *Nuclear Instruments and Methods* **118,** 177–182 (1974).

5. Reynes, J., Woignier, T. & Phalippou, J. Permeability measurement in composite aerogels: application to nuclear waste storage. *Journal of Non-Crystalline Solids* **285,** 323–327 (2001).

6. Woignier, T., Reynes, J., Phalippou, J., Dussossoy, J. . & Jacquet-Francillon, N. Sintered silica aerogel: a host matrix for long life nuclear wastes. *Journal of Non-Crystalline Solids* **225,** 353–357 (1998).

7. Guenther, U., Smirnova, I. & Neubert, R. H. H. Hydrophilic silica aerogels as dermal drug delivery systems – Dithranol as a model drug. *European Journal of Pharmaceutics and Biopharmaceutics* **69,** 935–942 (2008).

8. Smirnova, I., Suttiruengwong, S. & Arlt, W. Aerogels: Tailor-made Carriers for Immediate and Prolonged Drug Release. *KONA Powder Part. J.* (2005). at <http://www.kona.or.jp/search/23_086.pdf>

9. Gowers, S. L. & le Patourel, G. N. J. Toxicity of deposits of an amorphous silica

dust on different surfaces and their pick-up by Sitophilus granarius (L.) (Coleoptera: Curculionidae). *Journal of Stored Products Research* **20,** 25–29 (1984).

10. Westphal, A. J. *et al.* Aerogel keystones: Extraction of complete hypervelocity impact events from aerogel collectors. *Meteoritics & Planetary Science* **39,** 1375–1386 (2004).

11. Hörz, F. *et al.* Impact Features on Stardust: Implications for Comet 81P/Wild 2 Dust. *Science* **314,** 1716–1719 (2006).

12. Juzkow, M. Aerogel Capacitors Support Pulse, Hold-Up, and Main Power Applications. (2002). at <http://powerelectronics.com/portable_power_management/batteries/power_aerogel_capacitors_support/>

13. Vrieling, E. G., Beelen, T. P. M., van Santen, R. A. & Gieskes, W. W. C. Diatom silicon biomineralization as an inspirational source of new approaches to silica production. *Journal of Biotechnology* **70,** 39–51 (1999).

14. Cha, J. N., Stucky, G. D., Morse, D. E. & Deming, T. J. Biomimetic synthesis of ordered silica structures mediated by block copolypeptides. *Nature* **403,** 289–292 (2000).

15. Yang, H., Coombs, N. & Ozin, G. A. Morphogenesis of shapes and surface patterns in mesoporous silica. *, Published online: 17 April 1997; | doi:10.1038/386692a0* **386,** 692–695 (1997).

16. Kunz, W. & Kellermeier, M. Beyond Biomineralization. *Science* **323,** 344–345 (2009).

17. Voinescu, A. E. *et al.* Inorganic Self-Organized Silica Aragonite Biomorphic Composites. *Crystal Growth & Design* **8,** 1515–1521 (2008).

18. Kellermeier, M. *et al.* Additive-induced morphological tuning of self-assembled

silica–barium carbonate crystal aggregates. *Journal of Crystal Growth* **311,** 2530–2541 (2009).

19. Voinescu, A. E. *et al.* Co-precipitation of silica and alkaline-earth carbonates using TEOS as silica source. *Journal of Crystal Growth* **306,** 152–158 (2007).

20. Yang, Y., Suzuki, M., Owa, S., Shirai, H. & Hanabusa, K. Control of helical silica nanostructures using a chiral surfactant. *J. Mater. Chem.* **16,** 1644–1650 (2006).

21. Yang, Y., Suzuki, M., Owa, S., Shirai, H. & Hanabusa, K. Preparation of helical nanostructures using chiral cationic surfactants. *Chem. Commun.* 4462–4464 (2005). doi:10.1039/B508106H

22. Hanabusa, K., Hiratsuka, K., Kimura, M. & Shirai, H. Easy Preparation and Useful Character of Organogel Electrolytes Based on Low Molecular Weight Gelator. *Chem. Mater.* **11,** 649–655 (1999).

23. Smirnova, I., Suttiruengwong, S. & Arlt, W. Feasibility study of hydrophilic and hydrophobic silica aerogels as drug delivery systems. *Journal of Non-Crystalline Solids* **350,** 54–60 (2004).

24. Smirnova, I., Mamic, J. & Arlt, W. Adsorption of Drugs on Silica Aerogels. *Langmuir* **19,** 8521–8525 (2003).

25. Klamt, A., Eckert, F. & Diedenhofen, M. Prediction of Soil Sorption Coefficients with a Conductor-Like Screening Model for Real Solvents. (2002).

26. Mehler, C., Klamt, A. & Peukert, W. Use of COSMO-RS for the prediction of adsorption equilibria. *AIChE Journal* **48,** 1093–1099 (2002).

27. Wichmann, K., Diedenhofen, M. & Klamt, A. Prediction of Blood-Brain Partitioning and Human Serum Albumin Binding Based on COSMO-RS σ-Moments. *Journal of Chemical Information and Modeling* **47,** 228–233 (2007).

28. Klamt, A., Eckert, F. & Hornig, M. COSMO-RS: A novel view to physiological solvation and partition questions. *Journal of Computer-Aided Molecular Design* **15,** 355–365 (2001).

Appendices

Table of Figures

Figure 1: Publications per year for amorphous silica.....4

Figure 2: Publications per year for silica aerogels and silica xerogels.....5

Figure 3: The transparent aerogel on this balance weights only 518.3 mg.....7

Figures 4a and b: Showing thermal isolating properties of aerogel.....8

Figure 5: Showing a 2.5 kg brick on top of a 2 g aerogel.....9

Figures 6a and b: NASA stardust collector and particle captured in aerogel.....11

Figure 7: Reaction scheme for hydrolysation.....13

Figure 8: Reaction scheme showing the condensation reaction of fully hydrolysed silica with the so called lasso-chemistry.....13

Figures 9a and b: These diagrams show the evaporation of water from hydrogels. Phase I is dominated by the evaporation from the gel surface. Phase II has an additional transport of liquid from the inside of the gel resulting in shrinkage. Phase III shows occurrence of menisci in the gel pores when shrinkage stops. Phase IV shows evaporation of solvent inside the pores when transport to the gel surface lowers.....17

Figures 10a and b: Freeze drying device and freeze drying chamber.....18

Figure 11: Phase diagram of carbon dioxide.....19

Figure 12: Showing the assembled autoclave with teflon gaskets, windows and flanges in a side view.....25

Figure 13: Showing the assembled autoclave with teflon gaskets, windows and flanges from the top.....26

Figures 14a and b: Showing the front view of the autoclave without and with teflon

gasket.....26

Figures 15a and b: Showing the autoclave in front view with teflon gasket and window. Same view with the flange on top of the window.....27

Figures 16a and b: Isometric view of the autoclave without and with teflon gasket..27

Figures 17a and b: Isometric view of the autoclave with window and with window and flange on top of the Teflon gasket.....28

Figure 18: Showing the important parts of the supercritical drying device concerning the carbon dioxide flow.....30

Figures 19a and b: One of the analog pressure gauges. Digital ones where used additionally. A cooled high pressure liquid chromatography (HPLC) pump from Gilson was used for drying.....31

Figures 20a and b: Inside of the autoclave with the thermometer rod in the upper left. Heat control unit.....32

Figures 21: Not reproduceable ordered patterns of holes in silica aerogel.....37

Figure 22: Structure of the compound L-4PyCl.....38

Figure 23: Reaction scheme of step I.....39

Figure 24: Reaction scheme of step II.....39

Figure 25: Reaction scheme of step III.....40

Figure 26: Reaction scheme of step IV.....41

Figure 27: TGA of aerogel with organic remains from the template.....42

Figure 28: Gas chromatograph with auto-sampler and head-space auto-sampler.....46

Figure 29: BET ASAP 2000 from Micromeritics.....48

Figure 30: BET isotherms of heated aerogel and template modified heated aerogel. 49

Figures 31a and b: FT/IR-610 from Jasco.....50

Figure 32: Ultramicrotome for cutting epon slices.....52

Figure 33: Transmission electron microscope (TEM) FEI CM12.....53

Figure 34: Showing electron beam and signals.....55

Figures 35a and b: Scanning electron microscope (SEM) FEI Quanta 400 F with EDAX Genesis 2000 EDX System attached and (SEM) Zeis Gemini 1530. 56

Figure 36: TEM-micrographs of the surfactant templated aerogel as ground samples on carbon coated copper-grids. In the image on the right the twistings are marked.....58

Figure 37: TEM-micrographs of surfactant-free reference aerogels. The left microgrph shows a ground sample on a carbon coated copper-grid. The right micrograph consists of a ultrathin section of a sample embedded in the epoxy resin epon (thickness about 50nm).....59

Figure 38: TEM-micrographs of the modified aerogel embedded in epoxy resin epon as ultrathin sections of about 50nm thickness.....59

Figure 39: HR-SEM images of the template based aerogel (left image by Zeiss Ultra Plus, right image by Zeiss Gemini 1530).....60

Figure 40: HR-SEM images by Zeis Ultra Plus of the surfactant templated aerogel showing left handed fibres.....60

Figure 41: IR-spectra showing residual template surfactant L-4PyCl in the aerogels (AG).....62

Figures 42a and b: SEM-pictures of a freeze dried reference aerogel sample on the

left and a surfactant-templated freeze dried aerogel on the right side.....65

Figure 43: Digital image of (from left to right) surfactant-templated supercritically dried aerogel, surfactant-templated freeze dried aerogel, freeze dried reference aerogel and supercritically dried reference aerogel (transparent).66

Figure 44: Desorption of geraniol from geraniol loaded aerogels and liquid geraniol. 68

Figure 45: Showing the increased desorption rate of geraniol from aerogels with added water.....69

Figures 46a-d: Sigma-surfaces of water (upper left), acetonitrile (upper right), diethylether (lower left) and ethanol (lower right).....71

Figure 47: Showing sigma-profiles of some molecules. Certain molecules as ethanol have different possible conformations that result in different curves. The x-axis shows the electrostatic polarity σ of a certain surface fragment while the y-axis shows the number of occurances in the system. 73

Figure 48: Showing sigma-potentials of example molecules. The x-axis shows the electrostatic polarity sigma of a certain surface fragment while the y-axis shows the chemical potential in the system.....74

Figures 49: The figures show the predicted values compared to the actual measurements.....81

Figures 50: Showing the prediction errors compared to the actual measurements.....81

Figures 51a and b: Showing reference silica aerogel in the left and the modified silica aerogel in the right picture.....82

Figure 52: IR-spectra showing groups of SiOH at 957 1/cm and Si-O-Si at 1090 and 805 1/cm.....82

Figure 53: Top views onto the oxygen showing the σ-surface of H3SiOH on the left

and H3Si-O-SiH3 on the right.....83

Figures 54a and b: σ-profiles on the left side and σ-potentials on the right side of possible silica surface groups.....84

Sources and Copyright of some Figures:

Figures 4a and b: Showing thermal isolating properties of aerogel.….....8

4a: Source: https://commons.wikimedia.org/wiki/File:Aerogel_matches.jpg
Copyright: The image is in the public domain.
2012-12-10 18:03:46

4b: Source: https://en.wikipedia.org/wiki/File:Aerogelflower_filtered.jpg
Copyright: The image is in the public domain.
2012-12-10 18:03:52

Figure 5: Showing a 2.5 kg brick on top of a 2 g aerogel.….....9

Source: https://commons.wikimedia.org/wiki/File:Aerogelbrick.jpg
Copyright: The image is in the public domain.
2012-12-10 18:05:38

Figures 6a and b: NASA stardust collector and particle captured in aerogel.....……..11

6a: Source:
https://commons.wikimedia.org/wiki/File:Stardust_Dust_Collector_with_aerogel.jpg
Copyright: The image is in the public domain.
2012-12-10 18:05:48

6b: Source:
https://commons.wikimedia.org/wiki/File:Particle_captured_in_aerogel.jpg
Copyright: The image is in the public domain.
2012-12-10 18:05:43

Figure 11: Phase diagram of carbon dioxide.….....19

Source:
https://commons.wikimedia.org/wiki/File:Carbon_dioxide_pressure-temperature_phase_diagram.svg
Copyright: CC0 1.0 Universal Public Domain Dedication
2012-10-23 13:51:43

List of tables

Table 1: Supercritical conditions for various substances. Taken from the book Sol-Gel-Science (page 502).1.....20

Table 2: Element composition of the aerogel samples with and without surfactant loading before and after heat treatment.....61

Table 3: IR-spectra peaks and interpretation.....62

Table 4: BET results.....63

Table 5: Aerogel densities.....64

Table 6: Table showing the used and predicted values, the cross-validation test sets, and the training set of all values in their division into the used folds. Abbreviations: vap. p. vapor pressure, calc. calculated, acc acceptor, don donor, cv cross-validation, pred. predicted, mod. modified, and M molecular weight.....79

List of some Chemicals:

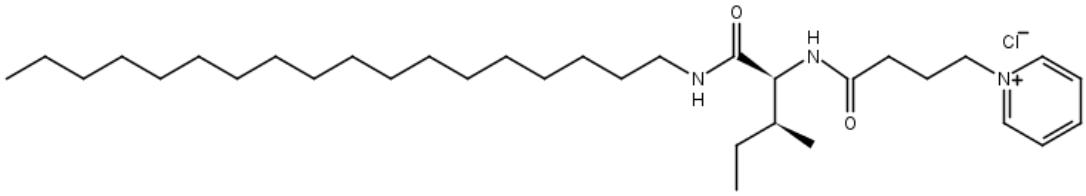

Surfactant L-4PyCl

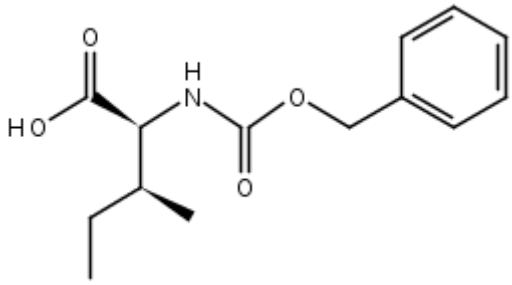

Z protected L-isoleucine

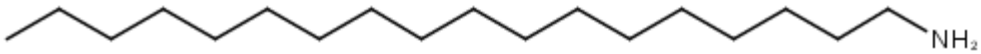

Octadecylamin

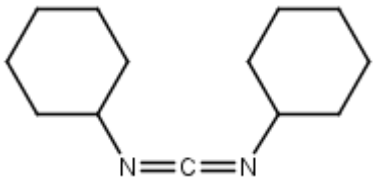

N,N'-dicyclohexylcarbodiimide (DCC)

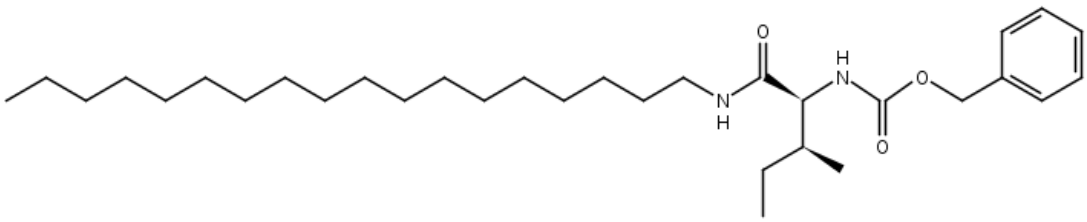

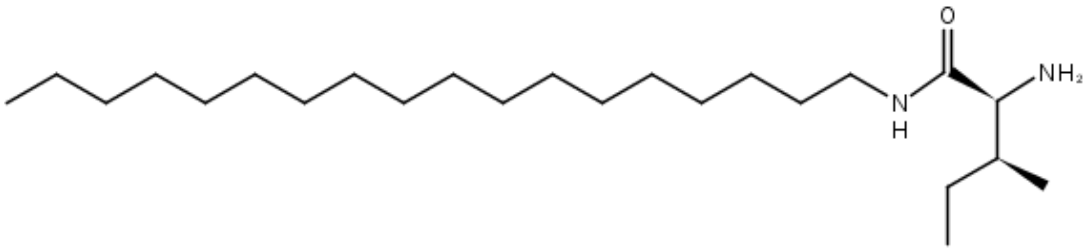

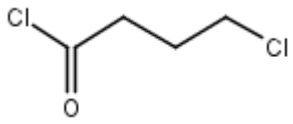

4-chlorobutyryl chloride

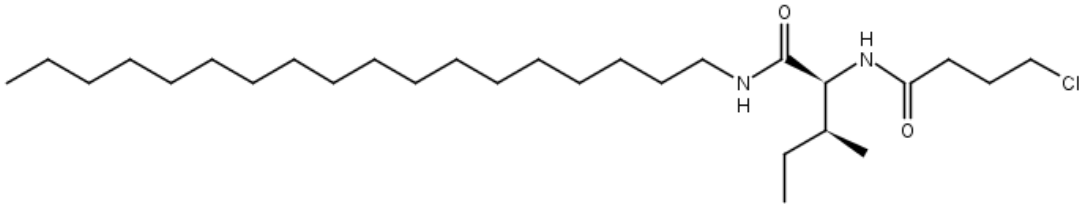

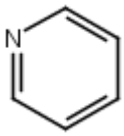

Pyridine

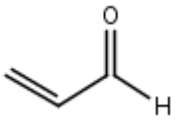

Acrolein

Eidesstattliche Erklärung

Ich erkläre hiermit an Eides statt, daß ich die vorliegende Arbeit ohne unzulässige Hilfe Dritter und ohne Benutzung anderer als der angegebenen Hilfsmittel angefertigt habe; die aus anderen Quellen direkt oder indirekt übernommenen Daten und Konzepte sind unter Angabe des Literaturzitats gekennzeichnet.

Bei der Auswahl und Auswertung folgenden Materials haben mir die nachstehend aufgeführten Personen in der jeweils beschriebenen Weise entgeltlich/unentgeltlich geholfen:

Siehe Danksagung (Acknowledgements).

Weitere Personen waren an der inhaltlich-materiellen Herstellung der vorliegenden Arbeit nicht beteiligt. Insbesondere habe ich hierfür nicht die entgeltliche Hilfe eines Promotionsberaters oder anderer Personen in Anspruch genommen. Niemand hat von mir weder unmittelbar noch mittelbar geldwerte Leistungen für Arbeiten erhalten, die im Zusammenhang mit dem Inhalt der vorgelegten Dissertation stehen.

Die Arbeit wurde bisher weder im In- noch im Ausland in gleicher oder ähnlicher Form einer anderen Prüfungsbehörde vorgelegt.